

Discovery of Ziresovir as a Potent, Selective and Orally Bioavailable Respiratory Syncytial Virus Fusion Protein Inhibitor

Xiufang Zheng, Lu Gao, Lisha Wang, Chungen Liang, Baoxia Wang, Yongfu Liu, Song Feng, Bo Zhang, Mingwei Zhou, Xin Yu, Kunlun Xiang, Li Chen, Tao Guo, Hong C Shen, Gang Zou, Jim Zhen Wu, and Hongying Yun

J. Med. Chem., **Just Accepted Manuscript** • DOI: 10.1021/acs.jmedchem.9b00654 • Publication Date (Web): 13 Jun 2019

Downloaded from <http://pubs.acs.org> on June 14, 2019

Just Accepted

“Just Accepted” manuscripts have been peer-reviewed and accepted for publication. They are posted online prior to technical editing, formatting for publication and author proofing. The American Chemical Society provides “Just Accepted” as a service to the research community to expedite the dissemination of scientific material as soon as possible after acceptance. “Just Accepted” manuscripts appear in full in PDF format accompanied by an HTML abstract. “Just Accepted” manuscripts have been fully peer reviewed, but should not be considered the official version of record. They are citable by the Digital Object Identifier (DOI®). “Just Accepted” is an optional service offered to authors. Therefore, the “Just Accepted” Web site may not include all articles that will be published in the journal. After a manuscript is technically edited and formatted, it will be removed from the “Just Accepted” Web site and published as an ASAP article. Note that technical editing may introduce minor changes to the manuscript text and/or graphics which could affect content, and all legal disclaimers and ethical guidelines that apply to the journal pertain. ACS cannot be held responsible for errors or consequences arising from the use of information contained in these “Just Accepted” manuscripts.

Discovery of Ziresovir as a Potent, Selective and Orally Bioavailable Respiratory Syncytial Virus Fusion Protein Inhibitor

Xiufang Zheng[†], Lu Gao[†], Lisha Wang[†], Chungeng Liang[†], Baoxia Wang[†], Yongfu Liu[†], Song Feng[†], Bo Zhang[†], Mingwei Zhou[†], Xin Yu[†], Kunlun Xiang[†], Li Chen[†], Tao Guo[‡], Hong C. Shen[†], Gang Zou[□], Jim Zhen Wu[□], and Hongying Yun^{†*}

[†]*Roche Pharma Research and Early Development, Roche Innovation Center Shanghai, Building 5, 720 Cailun Road, Shanghai, 201203 China*

[□]*Ark Biosciences Inc. 780 Cailun Road, Suite 701, ZhangJiang Hitech Park, Pudong, Shanghai, 201203 China*

[‡]*International Discovery Service Unit, Research Service Division, WuXi AppTec (Shanghai) Co., Ltd. Lane 31, Yiwei Road, Waigaoqiao, Shanghai, 200131 China*

KEYWORDS: *Respiratory Syncytial Virus (RSV), Antiviral, Fusion Inhibitors, Ziresovir, RO-0529, AK0529*

1
2
3 **ABSTRACT:** Ziresovir (RO-0529, AK0529) is reported here for the first time as a promising respiratory
4 syncytial virus (RSV) fusion (F) protein inhibitor that currently is in phase 2 clinical trials. This article
5 describes the process of RO-0529 as a potent, selective and orally bioavailable RSV F protein inhibitor,
6 and highlights the *in vitro* and *in vivo* anti-RSV activities and pharmacokinetics in animal species. RO-
7 0529 demonstrates single-digit nM EC₅₀ potency against laboratory strains as well as clinical isolates of
8 RSV in cellular assays, and more than one log viral load reduction in BALB/c mouse model of RSV viral
9 infection. RO-0529 was proven to be a specific RSV F protein inhibitor by identification of drug resistant
10 mutations of D486N, D489V, and D489Y in RSV F protein and the inhibition of RSV F protein-induced
11 cell-cell fusion in cellular assays.
12
13
14
15
16
17
18
19
20
21
22
23
24
25
26
27
28
29
30
31
32
33
34
35
36
37
38
39
40
41
42
43
44
45
46
47
48
49
50
51
52
53
54
55
56
57
58
59
60

Introduction

Human respiratory syncytial virus is a negative-sense single-stranded RNA virus and a member of the family of Pneumoviridae.¹ Human RSV infection causes acute upper and lower respiratory tract infection in infants, children, elderly, and immunocompromised adults. Particularly, all children by age of two will be infected by RSV and they can be re-infected in the succeeding RSV season.² RSV infection could be mild in healthy children and adults with symptoms of upper respiratory tract infection. However, in the high-risk populations, such as premature infants, immunocompromised adults, chronic obstructive pulmonary disease (COPD) and congestive heart failure (CHF) patients, upper respiratory tract infection can develop into lower respiratory tract infection, and associated mortality and morbidity would occur. The increased chance of morbidity or mortality is observed from severe RSV infection, causing bronchiolitis in infants and pneumonia in adult patients.^{2,3} The sequela of severe RSV infection in the children population could be recurrent wheezing or asthma.⁴ It should be noted that severe RSV infection causes around 3.4 million hospitalizations and around 160,000 deaths in children under 5 years old worldwide per year.^{5,6}

Ribavirin in an aerosol formulation is the only approved anti-RSV therapy. However, the limited efficacy and genotoxicity of the drug have hindered its application in clinic.⁷ There is no available vaccine for prophylaxis of RSV infection. Palivizumab was approved for passive prevention of RSV infection in high-risk infants, which reduces patient's hospitalization rate by only 50%. As a humanized monoclonal antibody against RSV fusion protein, Palivizumab exhibits no efficacy in the treatment of RSV infection.⁸ A safe and effective therapy is urgently needed for treatment of RSV infection.

RSV F protein is a glycoprotein expressed on the surface of viral envelope. It not only plays a crucial role for the virus entry but also promotes syncytia formation between the infected cells and the adjacent healthy cells.⁹ Inhibition of RSV F protein provided an opportunity to treat RSV infected patients. Small molecule F protein inhibitors are capable of decreasing the severity and duration of respiratory symptoms and cure the viral infection without the risk of prolonged hospitalization and complications.

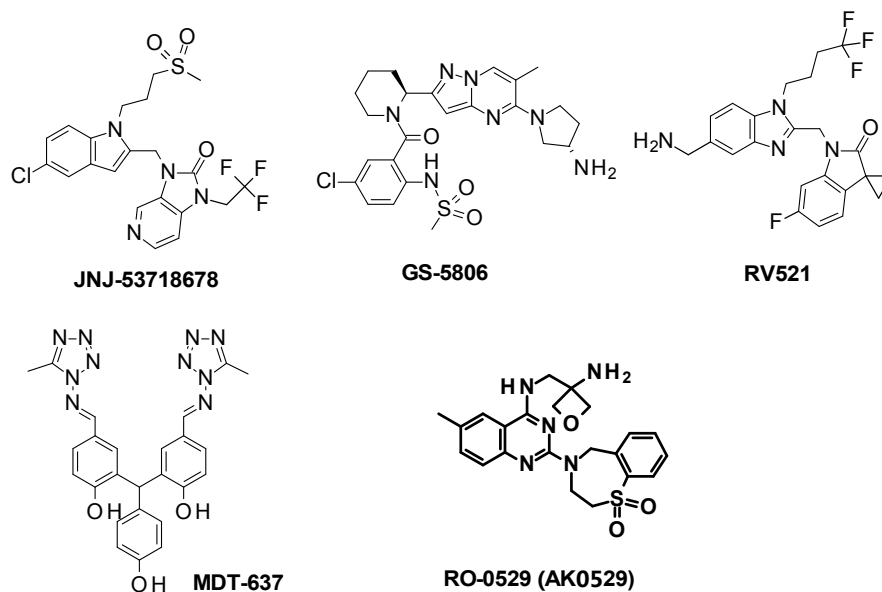


Figure 1. RSV Fusion Inhibitors in Clinical Development.

In the last two decades, several structurally different RSV F protein inhibitors have been discovered and reported,¹⁰⁻¹³ among of which several inhibitors had successfully progressed to clinical studies (Figure 1).¹⁴ JNJ-53718678 with a picomolar potency reduced viral load and clinical severity in a phase IIa human viral challenge study in healthy adults. Drug resistant mutation studies mapped its target on F protein.¹⁵ GS-5806, another picomolar F protein inhibitor, demonstrated efficacy in human RSV viral challenge studies by significantly reduction of viral load ($4.2 \log_{10}$) and disease symptom score.¹⁶ Drug resistant mutation studies proved its antiviral target as F protein.¹⁷ RV521, a single digital nanomolar F protein inhibitor, demonstrated good potency on the reduction of viral load and mucous production in a phase IIa human viral challenge study.¹⁸ VP-14637, an earlier generation of nanomolar F protein inhibitor, was formulated as an inhaled dry powder called MDT-637, and was tested in phase I clinical trial.¹⁹

We conducted a high throughput screen, identified a promising benzoazepinequinoline (BAQ) hit compound, and then underwent extensive lead identification to discover compound **1** as a promising lead compound (Figure 2).²⁰ In this article, we describe the discovery of Ziresovir (RO-0529, AK0529) as a

potent, selective and orally bioavailable RSV F protein inhibitor, which is currently in phase II clinical studies.²¹

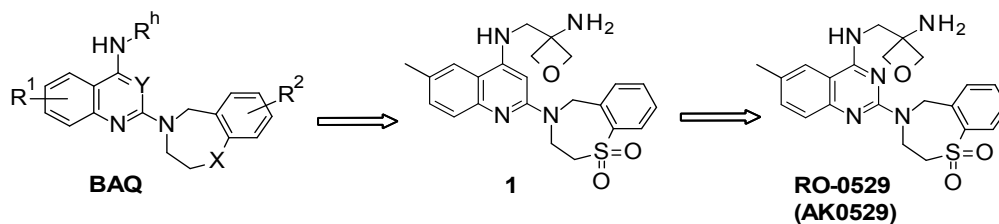
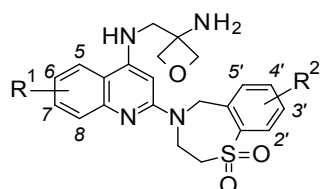


Figure 2. RO-0529 is originated from BAQ chemical series and optimized from Compound **1**.

Results and Discussion

As aforementioned, compound **1** was identified as a lead compound from the BAQ chemical series with a good potential to be a clinical development candidate. This compound showed good anti-RSV activity with EC₅₀ of 2 nM in CPE assay, and a much higher exposure (78-fold) in lung than plasma and good *in vivo* efficacy in an BALB/c mouse RSV infection model.²⁰ SAR exploration was conducted on the basis of compound **1**. We firstly modified the substitutions on quinoline (R¹) and benzoazepine (R²) (Table 1). As described in our previous work, 6-Me was very important for the anti-RSV activity (**1**). Replacement of 6-Me with 6-Cl significantly reduced anti-RSV activity (**1a**, EC₅₀=34 nM). Replacement of 6-Me with 6-CH₂OH (**1b**) maintained the activity but this compound did not possess cellular permeability. Introducing mono-F or di-F to quinoline led to a loss of anti-RSV activity (**1d-1f**). More potent compounds were discovered by substitution on R², such as **1j** and **1o** (EC₅₀=1 nM and 0.8 nM, respectively). Unfortunately, further study revealed a very higher human liver microsomal clearance for these two compounds.

Table 1. SAR of compound **1** analogues



Compd	R ¹	R ²	EC ₅₀ (μM) ^a	CC ₅₀ (μM)	TI ^b
1	6-Me	H	0.002	>100	>50,000
1a	6-Cl	H	0.034	87	2,560
1b	6-CH ₂ OH	H	0.002	>100	>50,000
1c	6-C(Me) ₂ OH	H	>100	>100	<1
1d	6-Me-7-F	H	0.021	64	3,050
1e	5-F-6-Me	H	0.023	93	4,040
1f	6-Me-7,8-di-F	H	0.51	53	104
1g	6-Me	2'-F	0.003	35	11,700
1h	6-Me	2'-OMe	0.35	>100	>286
1i	6-Me	3'-F	0.01	79	7,900
1j	6-Me	3'-OMe	0.001	92	92,000
1k	6-Me	3'-Me	0.005	91	18,200
1l	6-Me	3'-Cl	0.027	15	560
1m	6-Me	4'-F	0.072	93	1,290
1n	6-Me	4'-OMe	0.003	90	30,000
1o	6-Me	4'-OH	0.0008	>100	>125,000
1p	H	3'-OMe	0.008	>100	>12,500
1q	H	3'-Me	0.074	95	1,280

^a EC₅₀: the concentration of compound that reduced 50% cytopathic effect of RSV Long strain infected HEP-2 cells.

CC₅₀: the concentration of compound that manifests cytotoxicity towards 50% of uninfected HEP-2 cells. ^b

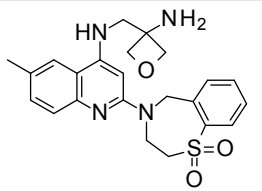
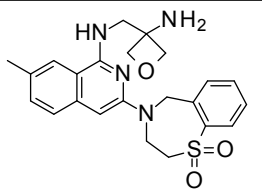
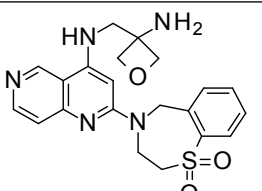
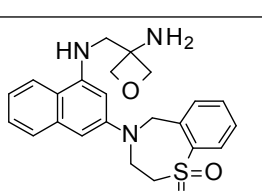
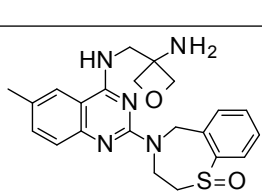
Therapeutic index (TI) is the ratio of CC₅₀/EC₅₀.

The next round of optimization was focused on the nitrogen walk of quinoline including removal or introduction of an additional nitrogen to quinoline (Table 2). Moving nitrogen from 1-position (**1**) to 3-position (**2a**) or adding one more nitrogen at 6-position (**2b**) of quinoline resulted in much decreased anti-

1
2
3 RSV activity. Converting quinoline (**1**) to naphthalene (**2c**) totally deprived the analog of anti-RSV activity.

4
5 Finally, converting quinoline to quinazoline led to the discovery of RO-0529, which demonstrated similar
6
7 anti-RSV activity ($EC_{50}=3$ nM) as compound **1**.
8
9

10
11 **Table 2. Nitrogen Walk around Quinoline of Compound 1^a**

14 Compd	R^h	EC₅₀ (μM)^a	CC₅₀ (μM)	TI^b
18 1		0.002	>100	>50,000
26 2a		0.22	81	370
34 2b		0.012	99	8,250
42 2c		>31.6	71	<2
50 RO-0529		0.003	>100	>33,300

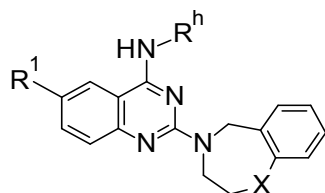
^a EC₅₀: the concentration of compound that reduced 50% cytopathic effect of RSV Long strain infected HEP-2 cells.

CC₅₀: the concentration of compound that manifests cytotoxicity towards 50% of uninfected HEP-2 cells. ^b

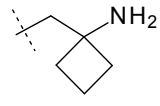
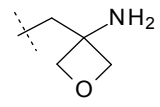
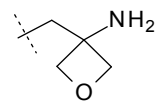
Therapeutic index (TI) is the ratio of CC₅₀/EC₅₀.

An SAR exploration on the quinazoline scaffold of RO-0529 was listed in Table 3. It was found that the SAR of quinazoline was very similar to quinoline (compound **1**). In the head portion (R^h), an oxetane substitution offered better anti-RSV activity than gem-di-Me (**3a**) and cyclobutyl (**3c**). Compared to cyclopropyl analog (**3b**), RO-0529 showed much larger TI (> 33,000 vs. 1,250). 6-Me demonstrated its importance for good anti-RSV activity compared to 6-H (**3d**, EC₅₀=20 nM). Although replacement of SO₂ with SO (**3e**) maintained the anti-RSV activity (EC₅₀=4 nM) and excellent TI, it was not further developed considering the oxidative conversion potential of SO (**3e**) to SO₂ in both *in vitro* and *in vivo* evaluation.

Table 3. SAR Exploration on the Scaffold Derived from RO-0529^a



Compd	R ^h	R ¹	X	EC ₅₀ (μM) ^a	CC ₅₀ (μM)	TI ^b
RO-0529		Me	SO ₂	0.003	>100	>33,000
3a		Me	SO ₂	0.016	20	1,250
3b		Me	SO ₂	0.004	13	3,250

3c		Me	SO ₂	0.10	21	210
3d		H	SO ₂	0.02	>100	>5,000
3e		H	SO	0.004	>100	>25,000

^a EC₅₀: the concentration of compound that reduced 50% cytopathic effect of RSV Long strain infected HEp-2 cells.

CC₅₀: the concentration of compound that manifests cytotoxicity towards 50% of uninfected HEp-2 cells. ^b Therapeutic index (TI) is the ratio of CC₅₀/EC₅₀.

Selection of RO-0529 as a clinical candidate:

Compound **1** and RO-0529 were both chosen as potential clinical candidates. In order to select a superior compound as the clinical candidate, we profiled both molecules in *in vitro* and *in vivo* anti-RSV activities, TI, DMPK and early safety profile. Between them, RO-0529 stood out.

Table 4 listed single dose pharmacokinetics (SDPK) results of compound **1** and RO-0529 in Sprague-Dawley rats. RO-0529 exhibited better oral exposure and bioavailability than compound **1**. Take all the results into consideration, RO-0529 was selected as the clinical candidate.

Table 4. Rat SDPK Profile of Compound 1 and RO5500529^a

Compound	1	RO-0529
Rat SDPK iv @ 2 mg/kg & po @10 mg/kg		
AUC_{0-24h} (po) (h*ng/mL)	442	906
<i>in vivo</i> CL (mL/min/kg)	51	58
T_{1/2, iv} (h)	1.7	1.2

V_{ss} (L/kg)	4.1	3.9
F (%)	13	32

^a The SDPK study in male Wistar-Han rats were carried out according to the standard procedures described in the supporting information. Plasma clearance (CL), volume of distribution at steady state (V_{ss}), area under the curve (AUC), oral bioavailability (F).

***In vitro* and *in vivo* anti-RSV activities of RO-0529**

RO-0529 was tested against RSV strains of both Long, A2 and B18537 subtypes in the CPE assay. It demonstrated high potency with EC₅₀ values in the single-digit nanomolar level (Table 5). In order to study the efficacy against clinical strains of RSV, clinical isolates of RSV A subtype (1177) and B subtype (821) were collected from Chongqing Children's Hospital in the RSV season from 2011 to 2012. In the cytopathic effect assays, both the drug showed similar activities in the clinical strains compared with laboratory strains of RSV (Long and B18537), which suggests that RO-0529 might be broadly active with a similar activity against both RSV A and B strains as well as clinical isolates (Table 5). RO-0529 showed no activity against influenza H1N1, human parainfluenza virus and rhinovirus in the CPE assay (data not shown), which indicates that its antiviral activity is RSV specific.

Table 5. Anti-RSV Activity of RO-0529^a

Antiviral assay	RSV Long CPE EC₅₀/EC₉₀ (μM)	RSV A2 CPE EC₅₀/EC₉₀ (μM)	RSV B18537 CPE EC₅₀/EC₉₀ (μM)	Clinical isolates Chongqing 1177 RSV A subtype CPE	Clinical isolates Chongqing 821 RSV B subtype CPE	RSV Long Plaque reduction EC₉₀ (μM)	Influenza H1N1 CPE EC₅₀ (μM)

				EC₅₀/EC₉₀	EC₅₀/EC₉₀		
				(μM)	(μM)		
RO-0529	0.003/0.005	0.002/0.003	0.002/0.003	0.004/0.007	0.003/0.008	0.010	> 100

^aEC₅₀: the concentration of compound that reduced 50% cytopathic effect of RSV Long and B strains in the presence of 10% FBS, plaque reduction in long strain and influenza H1N1 strain infected HEp-2 cells.

Furthermore, the effect of fetal bovine serum (FBS) on drug potency in the CPE assay using RSV Long strain was examined. The results indicated that there was no significant decrease in anti-RSV potency in the presence of 20% and 40% FBS (CPE EC₅₀/EC₉₀ = 0.003/0.008 μM with 40% FBS), comparing with potency under standard cell culture conditional in the presence of 10% FBS (Table 5).

In the CD-1 mice SDPK study, RO-0529 demonstrated a high tissue distribution to lung than plasma (Table 6). The lung exposure (AUC_(0-t)) is nearly 8-fold higher than that of plasma exposure. The T_{1/2} of lung is 3-time longer of that of plasma, suggesting a favorable lung targeted drug profile.

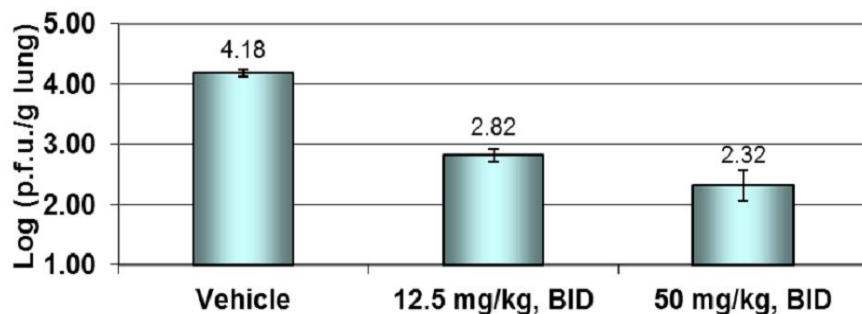
Table 6. CD-1 Mice SDPK Profile of RO-0529

PO (150 mg/kg/day)	AUC₍₀₋₂₄₎ (μg/L*h)	Tissue/plasma AUC₍₀₋₂₄₎ Ratio (μg/L*h)	T_{1/2} (h)	T_{max} (h)	C_{max} (μg/L)
Plasma	8,380	1	1.02	0.25	5,090
Lung	72,400	8.6	3.31	1	22,700

The *in vivo* efficacy against RSV was examined in female BALB/c mice. RO-0529 was orally dosed in 12 mice at 12.5 mg/kg and 50 mg/kg, twice a day (BID at 0 h and 8 h each day) for 4 days. It revealed that > 1 log unit of viral titer reduction in the lung of infected mice was achieved at the dose level

as low as 12.5 mg/kg. Further increase dose to 50 mg/kg can reduce viral titer to 1.9 log units compared to vehicle (Figure 4).

Figure 4. *In vivo* Reduction of RSV Titer in Mouse Lung with RO-0529^a



^a Female BALB/c mice were used for *in vivo* efficacy assay. Animals were anesthetized and to the animals were intranasally administrated RSV long strain (5×10^5 plaque-forming units [PFU]). After oral administration of RO-0529 BID for 4 days, the mice were euthanized with CO₂, and lungs were harvested and analyzed for viral titer.

The pharmacokinetics of RO-0529 was studied in mouse, rat, dog and monkey (Table 7). The *in vitro* liver microsomal clearance (Mic CL) and hepatocyte clearance (Hep CL) showed a good correlation using microsome preparations of mouse, rat and dog, respectively. In monkey and human, *in vitro* liver Mic CL was higher than Hep CL. The *in vivo* plasma clearance was much higher than liver blood flow in mouse, suggesting the possibility of high blood to plasma ratio, or extrahepatic metabolic clearance, such as urinary or biliary excretion. In general, the *in vitro* Hep CL and *in vivo* CL correlated well with each other in the rest of species, suggesting that the metabolic clearance is the major clearance pathway in the rat, dog, and monkey.

Table 7. Pharmacokinetics of RO-0529 in Nonclinical Species

Species	Liver Mic CL ^a (mL/min/kg)	Hep CL ^a (mL/min/kg)	<i>in vivo</i> CL (mL/min/kg)	V _{ss} (L/kg)	T _{1/2, iv} (h)	AUC _{0-24h, po} (ng*h/mL)	F%
CD-1 mouse ^b	74	60	277	6.3	0.4	1,970	66
SD rat ^b	40	42	58	3.9	1.2	906	32
Beagle dog ^c	12	10	36	6.7	2.8	1,170	26
Monkey ^c	40	23	26	1.9	1.0	1,440	22
Human	13	4.3	NA ^d	NA	NA	NA	NA

^a The *in vitro* microsomal CL and hepatocytes CL based on incubation with corresponding species microsomes and hepatocytes. ^b Mouse (5 mg/kg, iv; 50 mg/kg, po) and rat (2 mg/kg, iv; 10 mg/kg, po) SDPK with solution in 5% DMSO, 40% PEG400 and 55% 0.9% sodium chloride. ^c Beagle dog (1 mg/kg, iv; 10 mg/kg, po) and cynomolgus monkey (2 mg/kg, iv; 10 mg/kg, po) SDPK with solution in 12.5% captisol in water. Major parameters, including plasma clearance (CL), volume of distribution at steady state (V_{ss}), T_{1/2} (iv), area under the curve (AUC), and oral bioavailability (F) are reported. ^d NA: not available.

To identify the molecular target of the inhibitor, drug resistant mapping studies were performed, and drug resistant mutants were selected in the presence of RO-0529. Resistant viral isolates were obtained after several passages with increasing concentration of the compound. The RSV genome from the resistant isolates were amplified by reverse-transcription-PCR and sequenced in order to determine the viral protein that was targeted by the inhibitor. Each of the resistant isolates harbored a different single nucleotide substitution in the F gene, resulting in D486N, D489A, D489V, D489Y amino acid changes in passage 3, respectively. All the mutations rendered drug resistance to RO-0529 were located in the HRC region of the C-terminal of RSV-F protein. The data indicated that the bona fide target of RO-0529 is RSV F protein. The antiviral activity of RO-0529 was tested in the CPE assays using plaque-purified virus with D486N or D489A mutants. The results were shown in Table 8.

Table 8. Effect of RO-0529 on the Wild Type and Mutant Strains^a

CPE assay	EC ₅₀ /EC ₉₀ (μM) (WT)	EC ₅₀ /EC ₉₀ (μM) (D486N)	EC ₅₀ /EC ₉₀ (μM) (D489A)
RO-0529	0.003/0.005	>10/>10	2.1/10.0

^aFor the selected mutant strains of RSV, CPE assay was conducted as following. HEp-2 cells were seeded at 6000/well in 96-well plates. The viral inoculation volume was 50 μL and MOI was 0.04. The compound volume and the plates were read at absorbance of reagent CCK-8 at the absorbance of 450 nm/650 nm.

The mode of action of RO-0529 was further confirmed in an assay of inhibition of RSV F protein-induced cell-cell fusion process as shown in Figure 5. Without RO-0529, RSV F protein induced cell fusion process and generated syncytia formation shown in the red dot cycles (left figure). In the presence of 0.1 μM of RO-0529, the syncytia formation induced by the RSV F protein was completely inhibited (right figure). These results further confirmed that RO-0529 was a RSV F inhibitor, as there was no any other RSV viral protein present except F protein.

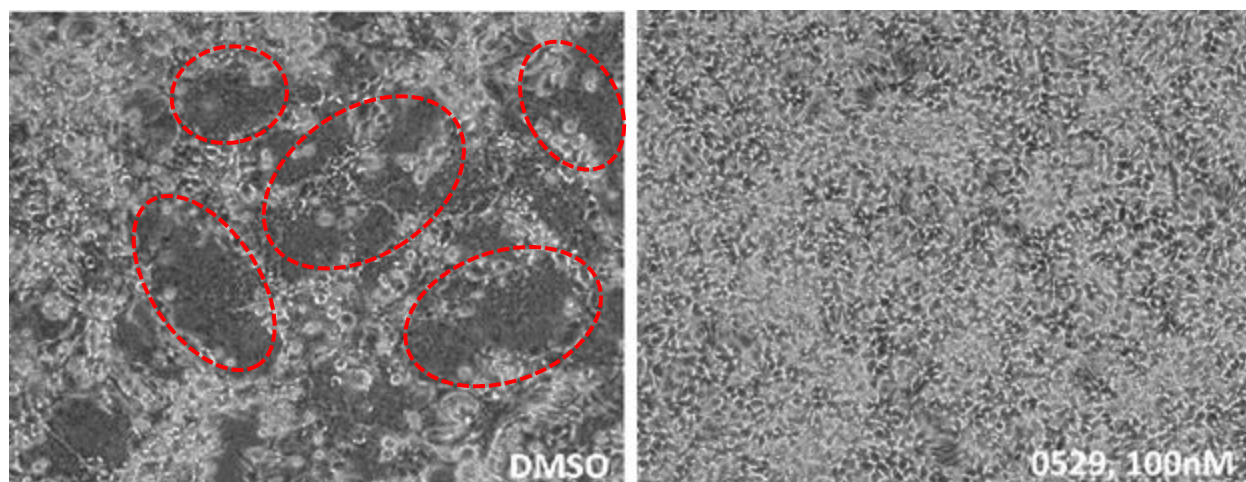


Figure 5. RO-0529 Inhibited RSV F Protein-induced Cell-Cell Fusion Process^a

^a RSV-F expression was induced by 1μg/ml tetracycline in the RSV F protein stable cell line. Compound was serial diluted and added into the RSV-F expressing cells. The cell-cell fusion was observed by microscopy at three days after compound addition.

Battles *et al*²² reported bona fide co-crystal structures for a number of RSV F inhibitors. All the RSV F inhibitors tested by Battles were found to target the same RSV F microdomain and the escape mutations observed in our study are known hot-spots of RSV pan-resistance to RSV F inhibitors. When

RO-0529 was docked into the same RSV F microdomain, it took the same binding mode as the Compound **1** in the previous article²⁰, which picks the similar interactions with the protein, such as the H-bond interaction with Asp486 and the hydrophobic interaction with Phe488. Since two N atoms of the oxetane side chain form the strong H-bond interaction with Asp486 (shown in orange in Figure 6a), the mutation of this residue – D486N, will significantly reduce the potency. In addition, the side chain of one Asp489 (shown in yellow in Figure 6a) forms the hydrophobic interaction with the 6-methyl of the quinazoline ring. Thus, mutations D489N & D489Y will also influence the potency of RO-0529. From these results, we conclude that the modeling and experimental results are highly corroborative.

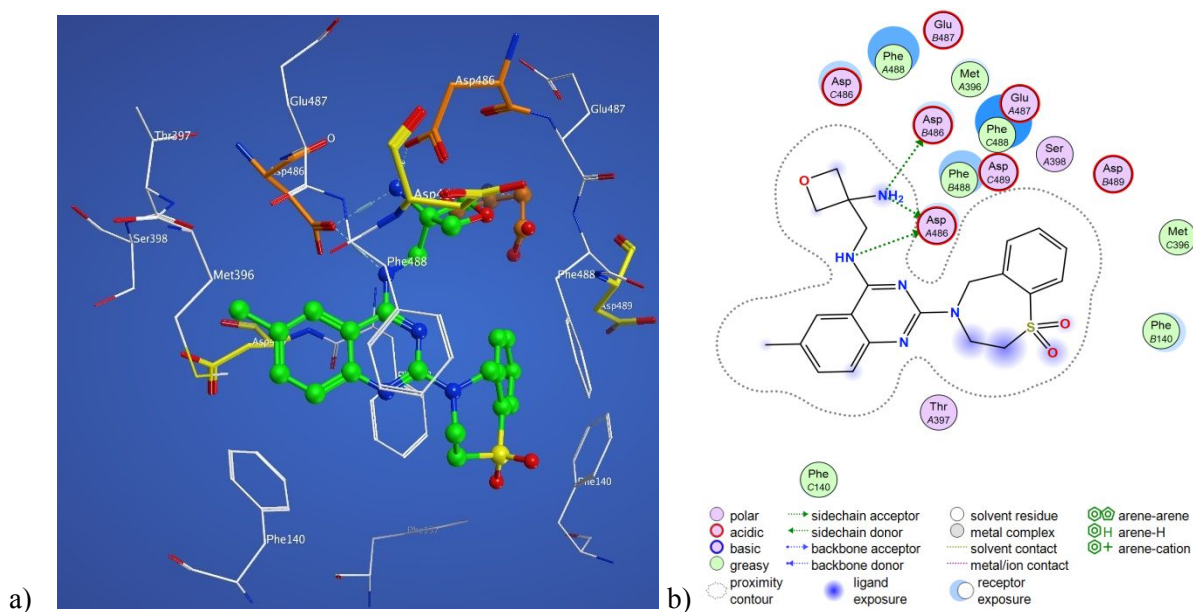


Figure 6. Docking Model of Compound RO-0529 Binding to a Three-fold Symmetric Cavity in Prefusion RSV F Protein.

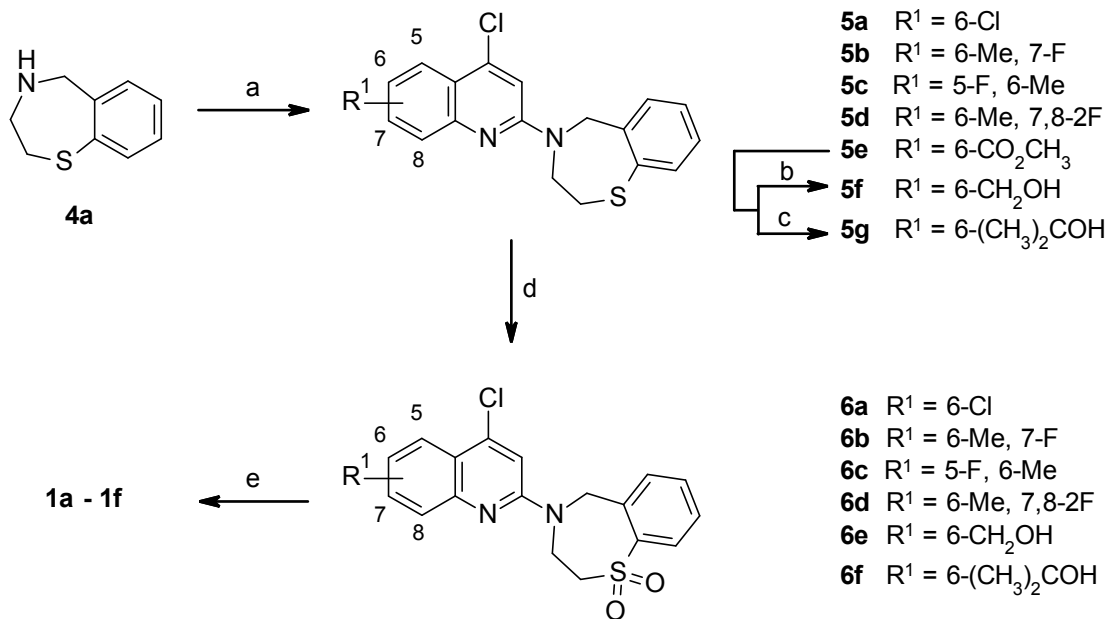
a) Side view of the RO-0529 in the binding pocket of prefusion FSV F glycoprotein (shown in white). Asp486 is shown as sticks with color in orange. Asp489 is shown as sticks with color in yellow. RO-0529 is shown in ball-and-stick mode, with carbon atoms colored in green, nitrogen atoms in blue, and oxygen atoms in red; b) 2D ligand-interaction diagram was generated in MOE. The interactions of compound RO-0529 with RSV F main-chain and side-chain atoms are shown as blue and green dotted lines, respectively. The arrowheads are pointed to the acceptor.

Clinical Development

In 2014, Ark Biosciences licensed RO-0529 from Roche for clinical development and renamed the drug as AK0529. Several clinical studies with the drug have been completed, including two Phase 1 clinical studies in healthy adult volunteers in Australia²³ and China²⁴, respectively, and a Phase 1 human mass balance study in the United Kingdom.²⁵ A global multi-center randomised double-blind placebo-controlled study of orally administered AK0529 is performed. This study evaluates the drug's safety, tolerability, pharmacokinetics, pharmacodynamics, and antiviral effect in infant patients hospitalized with RSV infection. The study is coded as Victor study, taking the term of "Viral Inhibition in Children for Treatment of RSV". WHO recently granted the common name of AK0529 as ziresovir. The final results of the VICTOR study will be reported in due course.

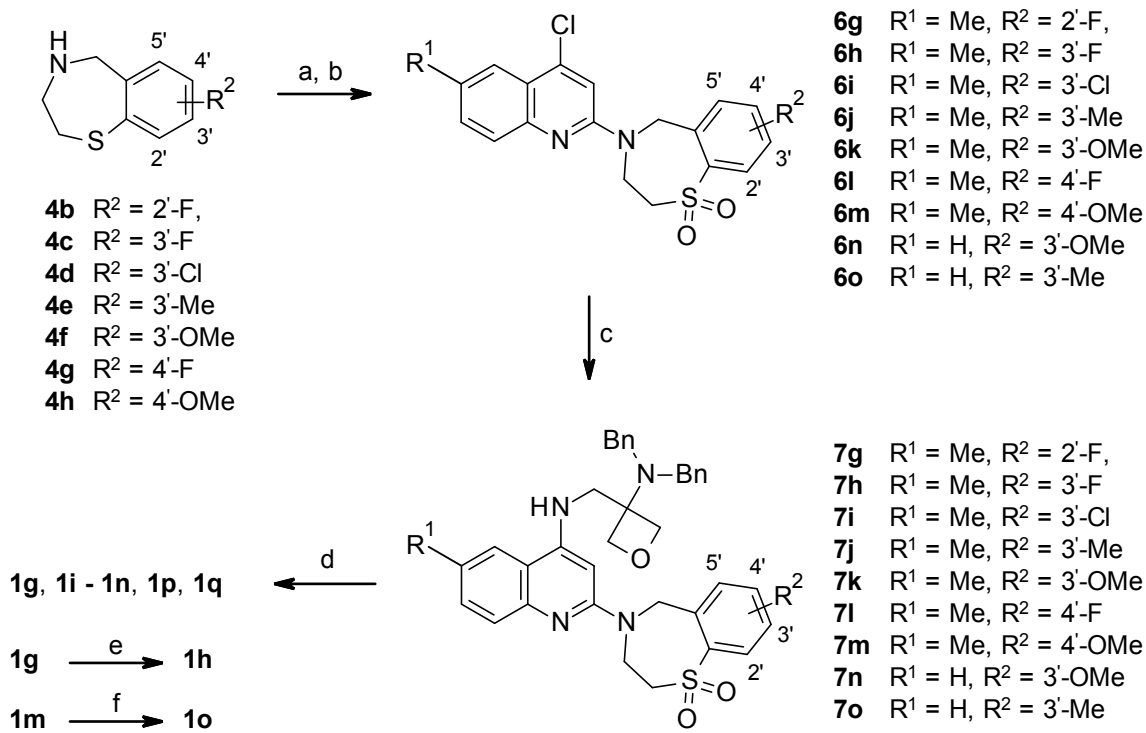
Chemistry

Scheme 1^a



^aReagents and conditions: (a) substituted 2,4-dichloroquinoline, 1-butanol, 160 °C, microwave; (b) LiAlH₄, THF, 0 °C to rt; (c) MeMgI, THF, 0 °C to rt; (d) *m*CPBA, DCM, 0 °C to rt; (e) 3-(aminomethyl)oxetan-3-amine, PdCl₂(dppf), dppf, *t*-BuONa, 1,4-dioxane, 120 °C, microwave.

Scheme 2^a

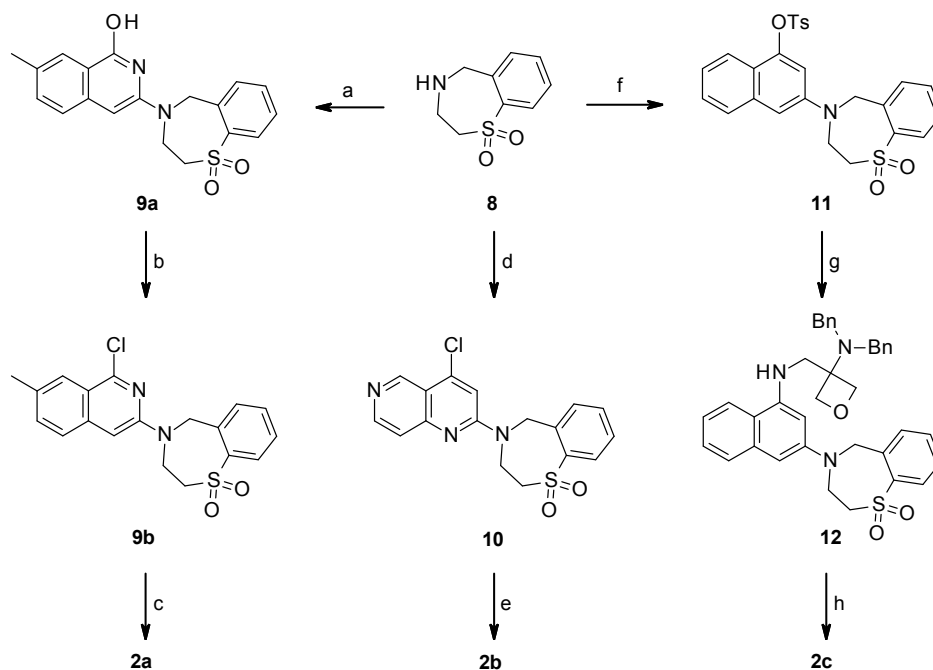


^aReagents and conditions: (a) substituted 2,4-dichloroquinoline, 1-butanol, 160 °C, microwave; (b) *m*CPBA, DCM, 0 °C to rt; (c) 3-(aminomethyl)-*N,N*-dibenzylloxetan-3-amine, Pd(OAc)₂, Cs₂CO₃, toluene, 120 °C; (d) Pd(OH)₂, H₂, TFA, MeOH, rt; (e) NaOMe, MeOH, 100 °C, microwave; (f) KOH, DMSO, 100 °C, microwave.

Compound **1**, and intermediates **4a** and **8** were prepared as described previously.²⁰ Compounds **1a–1f** were prepared as shown in Scheme 1, and compounds **1g–1q** were prepared as shown in Scheme 2. Intermediates **5a–5g** were prepared starting from the 1,4-benzothiazepine **4a**. S_NAr reactions with the substituted 2,4-dichloroquinolines led to **5a–5e**. Compound **5e** was derivatized to alcohols **5f** and **5g** by reduction and dimethylation, respectively. These intermediates were then oxidated to the corresponding sulfones **6a–6f** with *m*CPBA, followed by Buchwald-Hartwig coupling with 3-(aminomethyl)oxetan-3-amine to afford compounds **1a–1f**. Coupling of 2,4-dichloroquinolines with substituted 1,4-benzothiazepines **4b–4h** (see Supporting Information for their synthesis), followed by oxidation to afford intermediates **6g–6o**. The subsequent coupling reactions with 3-(aminomethyl)-*N,N*-dibenzylloxetan-3-amine generated **7g–7o**, and finally de-benzylation afforded the final compounds **1g, 1i–1o, 1p** and **1q**.

Compounds **1h** and **1o** were obtained by further displacement of the corresponding F substituted **1g** and **1m**, respectively.

Scheme 3^a

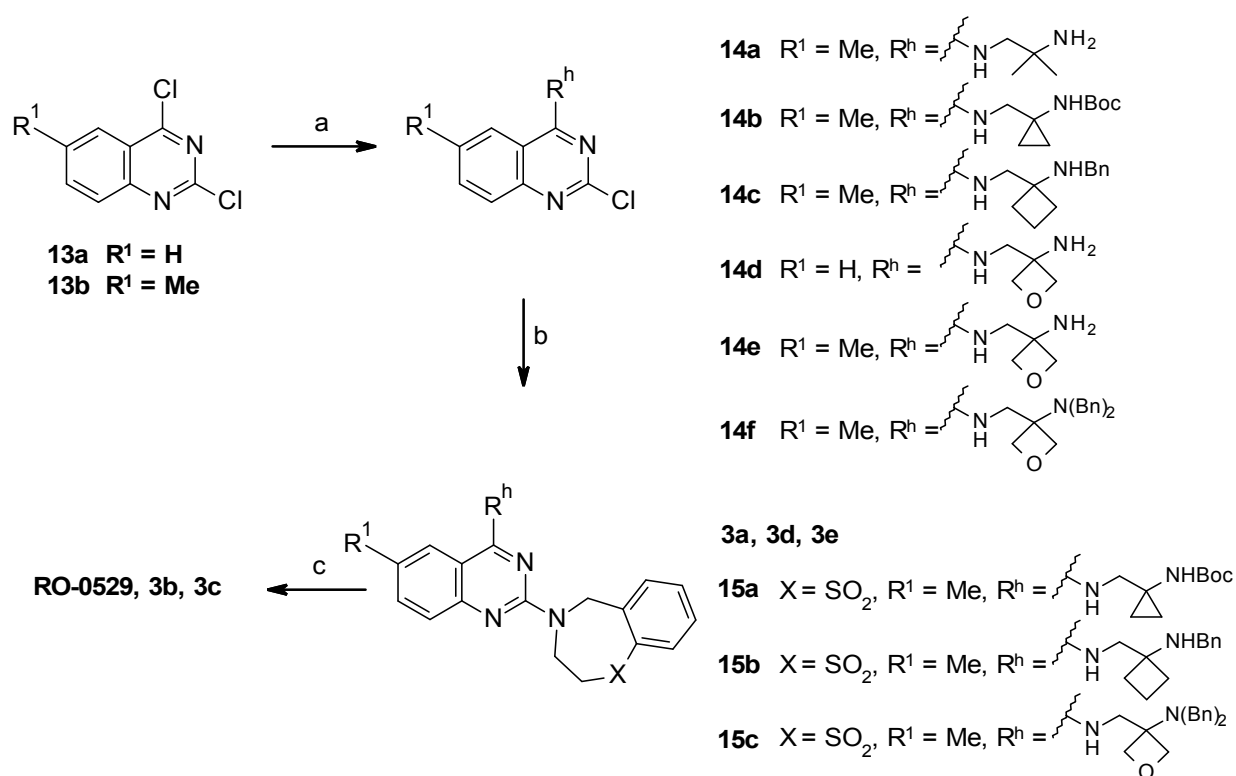


^aReagents and conditions: (a) 2-(cyanomethyl)-5-methyl-benzoic acid, DMA, 170 °C; (b) POCl₃, reflux; (c) 3-(aminomethyl)oxetan-3-amine, PdCl₂(dppf), dppf, *t*-BuONa, 1,4-dioxane, 150 °C, microwave; (d) 2,4-dichloro-1,6-naphthyridine, 1-butanol, 160 °C, microwave; (e) 3-(aminomethyl)oxetan-3-amine, PdCl₂(dppf), dppf, *t*-BuONa, 1,4-dioxane, 120 °C, microwave; (f) [3-(trifluoromethylsulfonyloxy)-1-naphthyl] 4-methylbenzenesulfonate, Pd₂(dba)₃, dppf, *t*-BuONa, toluene, 110 °C, microwave; (g) 3-(aminomethyl)-*N,N*-dibenzylloxetan-3-amine, Pd(*t*-Bu₃P)₂, Josiphos SL-J003-1, *t*-BuONa, toluene, 120 °C, microwave; (h) Pd(OH)₂, H₂, TFA, MeOH, rt.

Compounds **2a–2c** (Table 2) were made as shown in Scheme 3. Reaction of intermediate **8** with 2-(cyanomethyl)-5-methyl-benzoic acid led to **9a**, which was then converted to chloride **9b**. The coupling with 2,4-dichloro-1,6-naphthyridine or [3-(trifluoromethylsulfonyloxy)-1-naphthyl] 4-methylbenzenesulfonate gave intermediate **10** or **11**, respectively. Buchwald-Hartwig coupling with 3-

(aminomethyl)oxetan-3-amine led directly to compounds **2a** and **2b**, and with 3-(aminomethyl)-*N,N*-dibenzylloxetan-3-amine followed by de-benzylated led to compound **2c**.

Scheme 4^a



^aReagents and conditions: (a) amine, Et₃N, MeOH, rt; (b) Compounds **3a** and **15b**: (i) **4a**, 1-butanol, 160 °C, microwave; (ii) *m*CPBA, DCM, 0 °C to rt; Compounds **3d** and **15c**: **8**, Et₃N, DMF, 130 °C, microwave; Compound **3e**: 2,3,4,5-tetrahydro-1,4-benzothiazepine 1-oxide, 1-butanol, 160 °C, microwave; Compound **15a**: **8**, NH₄Cl, EtOH, 70 °C; (c) Compounds RO-0529 and **3c**: Pd(OH)₂, H₂, TFA, MeOH, rt; Compound **3b**: TFA, DCM, rt.

In Scheme 4, 2,4-dichloroquinazoline **13** was used as the starting material for the synthesis of **3a–3e** and RO-0529 (Table 3). Displacement of the 4-Cl in **13** with different amines generated intermediates **14a–14f** in high yield which were then coupled with the corresponding intermediates **8** and 2,3,4,5-tetrahydro-1,4-benzothiazepine 1-oxide to afford **3d, 3e, 15a and 15c** directly, and with **4a** followed by oxidation with

1
2
3 *m*CPBA to generate **3a** and **15b**. Finally, deprotection of **15a–15c** resulted in the final compounds **3b**, **3c**
4
5 and RO-0529.
6
7
8
9

10 11 **Conclusions**

12
13
14 In summary, ziresovir (RO-0529, AK0529) is evolved from compound **1**, which was a lead
15
16 compound from the benzoazepine quinoline (BAQ) series discovered from a high throughput screen hit.
17
18 Although the difference of ziresovir and compound **1** is quite minor with only replacement of quinoline
19
20 with quinazoline moiety, the DMPKT properties are quite different between these two compounds.
21
22 Ziresovir demonstrates a larger safety window with the preferred pharmacokinetics compared to compound
23
24 **1**. As we had interpreted in the previous publication²⁰, the introduction of oxetane to control basicity of the
25
26 terminal amine in the head portion is the highlight of the discovery efforts, which is important to reduce the
27
28 V_{ss} with intact anti-RSV activity. Ziresovir demonstrated good *in vitro* antiviral activity to both RSV A and
29
30 B strains. In addition, it also demonstrated comparable antiviral activity to clinical isolated RSV strains
31
32 tested thus far. Due to the higher lung exposure, it demonstrated a good *in vivo* efficacy in the mice RSV
33
34 viral challenge model. In the drug resistant mutation selection study, D486N, D489V and D489Y in RSV
35
36 F protein were identified as the resistant viruses, which confirmed drug's mechanism of action of targeting
37
38 RSV fusion protein. With the good and balanced preclinical profile of antiviral, DMPK and toxicology
39
40 properties, ziresovir has since moved to clinical development. The clinical results will be reported in due
41
42 course.
43
44
45

46 47 **EXPERIMENTAL SECTION**

48
49
50 **Synthetic Chemistry General Comments.** Intermediates and final compounds were purified by flash
51
52 chromatography using one of the following instruments: (i) Biotage SP1 system and the Quad 12/25
53
54 cartridge module; (ii) ISCO Combi-flash chromatography instrument. Silica gel brand and pore size: (i)
55
56
57
58
59
60

1
2
3 KP-SIL 60 Å, particle size 40–60 μm; (ii) CAS registry no., silica gel, 63231-67-4, particle size 47–60 μm
4 silica gel; (iii) ZCX from Qingdao Haiyang Chemical Co., Ltd., pore 200–300 or 300–400. Intermediates
5 and final compounds were purified by preparative HPLC on reversed phase column using XBridge Perp
6 and final compounds were purified by preparative HPLC on reversed phase column using XBridge Perp
7 C₁₈ (5 μm, OBD 30 mm × 100 mm) column or SunFire Perp C₁₈ (5 μm, OBD 30 mm × 100 mm) column.
8
9

10
11 LC/MS spectra were obtained using a MicroMass Platform LC (Waters Alliance 2795-ZQ2000).
12 Standard LC/MS conditions were as follows (running time 6 min). Acidic condition: A, 0.1% formic acid
13 in H₂O; B, 0.1% formic acid in acetonitrile. Basic condition: A, 0.01% NH₃·H₂O in H₂O; B, acetonitrile.
14 Neutral condition: A, H₂O; B, acetonitrile. Mass spectra (MS): Generally only ions which indicate the
15 parent mass are reported, and unless otherwise stated the mass ion quoted is the positive mass ion (M+H)⁺.
16
17
18
19
20
21

22 The microwave assisted reactions were carried out in a Biotage Initiator Sixty. NMR spectra were
23 obtained using Bruker Avance 400 MHz. All reactions involving air-sensitive reagents were performed
24 under an argon atmosphere. Reagents were used as received from commercial suppliers without further
25 purification unless otherwise noted. All of the final compounds had purities greater than 95% based upon
26 HPLC, LC/MS, and ¹H NMR analyses. All of the reported yields are for isolated products and are not
27 optimized.
28
29
30
31
32
33

34
35
36 ***N*-[(3-Aminooxetan-3-yl)methyl]-6-chloro-2-(1,1-dioxido-2,3-dihydro-1,4-benzothiazepin-4(5*H*)-**
37 ***yl*)quinolin-4-amine (1a).** To a solution of 2,4,6-trichloroquinoline (2 g, 8.6 mmol) in 20 mL of 1-butanol
38 was added 6,7,8,9-tetrahydro-5-thia-8-aza-benzocycloheptene (**4a**, 1.42 g, 8.6 mmol). The mixture was
39 stirred at 160 °C under microwave irradiation for 2 h. After being cooled to room temperature, the mixture
40 was diluted with saturated NaHCO₃ and extracted with DCM (50 mL). The organic layer was washed with
41 brine, dried over Na₂SO₄. The solvent was evaporated under reduced pressure, and the residue was purified
42 by flash column, eluting with a gradient of 0–10% MeOH in DCM to give compound **5a** as a light yellow
43 solid (2.2 g, yield 71%), which was used for the next step directly.
44
45
46
47
48
49
50
51

52
53 To a solution of compound **5a** (3 g, 8.31 mmol) in DCM (50 mL) was added *m*CPBA (3.6 g, 20.78 mmol)
54 at 0 °C. After the addition, the resulting mixture was stirred for 1 h while allowing the temperature to rise
55
56
57
58
59
60

1
2
3 slowly to room temperature. The reaction mixture was quenched with saturated Na₂SO₃ and then washed
4 sequentially with saturated Na₂CO₃ (30 mL) and saturated brine (30 mL). The organic layer was dried over
5 Na₂SO₄, filtered, and then concentrated *in vacuo*. The residue was purified by flash column, eluting with a
6 gradient of 0–10% MeOH in DCM to give compound **6a** as a white solid (2.7 g, yield 83%), which was
7 used for the next step directly.
8
9

10
11
12
13
14 A mixture of compound **6a** (539 mg, 1.37 mmol), PdCl₂(dppf) (100 mg, 0.14 mmol), dppf (76 mg, 0.14
15 mmol), *t*-BuONa (263 mg, 2.74 mmol) and 3-(aminomethyl)oxetan-3-amine (140 mg, 1.37 mmol) in 1,4-
16 dioxane (10 mL) was stirred at 120 °C under microwave irradiation for 1.5 h. The resulting mixture was
17 concentrated *in vacuo* and purified by preparative HPLC to afford compound **1a** (70 mg, yield 11%). MS
18 obsd (ESI⁺) [(M+H)⁺] 459. ¹H NMR (400 MHz, CD₃OD) δ ppm 8.34 (s, 1H), 8.00–8.02 (t, *J* = 4.0, 2.4 Hz,
19 2H), 7.90–7.92 (d, *J* = 7.2 Hz, 1H), 7.62–7.65 (m, 1H), 7.54–7.56 (d, *J* = 9.2 Hz, 1H), 7.44–7.49 (m, 2H),
20 6.27 (s, 1H), 5.22 (s, 2H), 4.63–4.67 (m, 4H), 4.56 (br s, 2H), 3.78 (s, 2H), 3.60–3.63 (t, *J* = 4.8 Hz, 2H).
21
22
23
24
25
26
27
28
29

30 Compounds **1b–1f** were prepared by a similar procedure to that described for compound **1a** (Scheme 1).
31
32

33
34 **[4-[(3-Aminooxetan-3-yl)methyl]amino]-2-(1,1-dioxido-2,3-dihydro-1,4-benzothiazepin-4(5H)-**
35 **yl)quinolin-6-yl]methanol (1b)**. MS obsd (ESI⁺) [(M+H)⁺] 455. HRMS calcd [(M+H)⁺] 455.1753,
36 measured [(M+H)⁺] 455.1754. ¹H NMR (400 MHz, CD₃OD) δ ppm 8.33 (br s, 1H), 8.02–8.11 (m, 2H),
37 7.93 (d, *J* = 7.33 Hz, 1H), 7.65–7.76 (m, 3H), 7.55 (t, *J* = 7.71 Hz, 1H), 6.26 (s, 1H), 5.32 (s, 2H), 4.72 (s,
38 2H), 4.63 (s, 4H), 4.57 (br s, 2H), 3.88 (s, 2H), 3.72 (br s, 2H).
39
40
41
42
43
44

45 **2-[4-[(3-Aminooxetan-3-yl)methylamino]-2-(1,1-dioxo-3,5-dihydro-2H-1λ6,4-benzothiazepin-**
46 **4-yl)-6-quinoly]propan-2-ol (1c)**. MS obsd (ESI⁺) [(M+H)⁺] 483. HRMS calcd [(M+H)⁺] 483.2066,
47 measured [(M+H)⁺] 483.2066. ¹H NMR (400 MHz, CDCl₃) δ ppm 8.05 (dd, *J* = 1.26, 7.83 Hz, 1H), 7.69–
48 7.73 (m, 2H), 7.58–7.62 (m, 1H), 7.50–7.57 (m, 2H), 7.39 (dt, *J* = 1.26, 7.71 Hz, 1H), 6.04 (s, 1H), 5.51 (br
49 s, 1H), 5.16 (s, 2H), 4.56–4.63 (m, 4H), 4.45–4.71 (br s, 2H), 3.60 (d, *J* = 4.80 Hz, 4H), 1.62 (s, 6H).
50
51
52
53
54
55
56
57
58
59
60

1
2
3 ***N*-[(3-Aminooxetan-3-yl)methyl]-2-(1,1-dioxido-2,3-dihydro-1,4-benzothiazepin-4(5*H*)-yl)-7-fluoro-**
4 **6-methylquinolin-4-amine (1d).** MS obsd (ESI+) [(M+H)⁺] 457. HRMS calcd [(M+H)⁺] 457.1710,
5 measured [(M+H)⁺] 457.1709. ¹H NMR (400 MHz, CD₃OD) δ ppm 8.03–8.05 (d, *J* = 8.0 Hz, 1H), 7.88–
6 7.92 (t, *J* = 8.0, 8.8 Hz, 2H), 7.65–7.68 (m, 1H), 7.49–7.53 (t, *J* = 7.6 Hz, 1H), 7.25–7.28 (d, *J* = 11.6 Hz,
7 1H), 6.20 (s, 1 H), 5.24 (s, 2 H), 4.48–4.66 (m, 6 H), 3.82 (s, 2 H), 3.64–3.66 (m, 2 H), 2.68 (s, 3 H).
8
9
10
11
12
13

14 ***N*-[(3-Aminooxetan-3-yl)methyl]-2-(1,1-dioxido-2,3-dihydro-1,4-benzothiazepin-4(5*H*)-yl)-5-fluoro-**
15 **6-methylquinolin-4-amine (1e).** MS obsd (ESI+) [(M+H)⁺] 457. HRMS calcd [(M+H)⁺] 457.1710,
16 measured [(M+H)⁺] 457.1716. ¹H NMR (400 MHz, DMSO-*d*₆) δ ppm 7.97–7.99 (d, *J* = 7.2 Hz, 1H), 7.88–
17 7.90 (m, 1H), 7.62–7.66 (m, 1H), 7.47–7.51 (t, *J* = 7.6 Hz, 1H), 7.24–7.29 (t, *J* = 8.4, 8.8 Hz, 1H), 7.18–
18 7.20 (d, *J* = 8.4 Hz, 1H), 6.57–6.61 (d, *J* = 16.0 Hz, 1H), 6.12 (s, 1H), 5.11 (s, 2H), 4.43–4.44 (d, *J* = 6.0
19 Hz, 2H), 4.37–4.38 (d, *J* = 6.0 Hz, 2H), 3.61–3.63 (t, *J* = 4.4, 4.8 Hz, 2H), 3.53 (s, 2H), 2.67–2.68 (t, *J* =
20 2.0, 1.6 Hz, 1H), 2.33–2.34 (t, *J* = 2.0, 1.6, 1H), 1.92 (s, 3H).
21
22
23
24
25
26
27
28
29

30 ***N*-[(3-Aminooxetan-3-yl)methyl]-2-(1,1-dioxido-2,3-dihydro-1,4-benzothiazepin-4(5*H*)-yl)-7,8-**
31 **difluoro-6-methylquinolin-4-amine (1f).** MS obsd (ESI+) [(M+H)⁺] 475. HRMS calcd [(M+H)⁺]
32 475.1615, measured [(M+H)⁺] 475.1622. ¹H NMR (400 MHz, DMSO-*d*₆) δ ppm 8.04 (br s, 1H), 7.88 (d, *J*
33 = 7.83 Hz, 2H), 7.62 (t, *J* = 6.82 Hz, 1H), 7.47 (t, *J* = 7.58 Hz, 1H), 7.18 (br s, 1H), 6.31 (br s, 1H), 5.16
34 (br s, 2H), 4.60 (d, *J* = 8.34 Hz, 2H), 3.97–4.05 (m, 2H), 3.82 (br s, 2H), 3.62 (br s, 2H), 3.17 (m, 2H), 2.33
35 (s, 3H).
36
37
38
39
40
41
42
43

44 ***N*-[(3-Aminooxetan-3-yl)methyl]-2-(9-fluoro-1,1-dioxido-2,3-dihydro-1,4-benzothiazepin-4(5*H*)-yl)-**
45 **6-methylquinolin-4-amine (1g).** A mixture of 9-fluoro-2,3,4,5-tetrahydro-1,4-benzothiazepine (**4b**, 0.59
46 g, 3.2 mmol), 2,4-dichloro-6-methyl-quinoline (0.68 g, 3.2 mmol) and 1-butanol (4 mL) was stirred at 160
47 °C under microwave irradiation for 2.5 h. The solvent was removed, and the residue was dissolved in a
48 mixture solvent of EtOH and DCM. After the DCM in the resulting mixture was removed under reduced
49 pressure, the resulting precipitate was collected by filtration, which was washed with diethyl ether and
50
51
52
53
54
55
56
57
58
59
60

1
2
3 petroleum ether, dried *in vacuo* to afford 4-(4-chloro-6-methyl-2-quinoly)-9-fluoro-3,5-dihydro-2*H*-1,4-
4 benzothiazepine as a pale white solid (0.57 g, yield 50%). MS obsd (ESI+) [(M+H)⁺] 359.

8 A mixture of 4-(4-chloro-6-methyl-2-quinoly)-9-fluoro-3,5-dihydro-2*H*-1,4-benzothiazepine (0.39 g, 1.1
9 mmol) and NaIO₄ (0.71 g, 3.3 mmol) in MeOH (15 mL) and water (6 mL) was stirred at room temperature
11 for 12 h. After removal of the solvent, the residue was dissolved into MeOH (15 mL), then cooled to 0 °C.
12 A solution of KMnO₄ (0.17 g, 1.1 mmol) in water (6 mL) was added dropwise. After being stirred at 0 °C
14 for 2 h, the mixture was extracted with EtOAc. The organic layer was filtered through a pad of silica gel,
17 concentrated *in vacuo* to give compound **6g** (0.40 g, yield 93%), which was used for the next step directly.
19 MS obsd (ESI+) [(M+H)⁺] 391.

23 A mixture of compound **6g** (250 mg, 0.64 mmol), Cs₂CO₃ (420 mg, 1.28 mmol), Pd(OAc)₂ (14.4 mg, 0.064
25 mmol), and 3-(aminomethyl)-*N,N*-dibenzylloxetan-3-amine (270 mg, 0.96 mmol) in toluene (10 mL) was
27 stirred at 120 °C for 4 h. After being concentrated under reduced pressure, the residue was purified by flash
29 column, eluting with 5% MeOH and 0.5% Et₃N in DCM to afford compound **7g** (200 mg, yield 50%).
31 MS obsd (ESI+) [(M+H)⁺] 637.4.

35 A mixture of compound **7g** (200 mg, 0.31 mmol), palladium hydroxide (10% on carbon, 100 mg) and TFA
37 (0.2 mL) in MeOH (20 mL) was stirred under a hydrogen atmosphere for 12 h. After being basified with
39 saturated NaHCO₃, the mixture was extracted with DCM. The organic layer was dried over anhydrous
41 Na₂SO₄ and concentrated under reduced pressure. The residue was purified by HPLC to afford compound
43 **1g** as a white solid (20 mg, yield 14%). MS obsd (ESI+) [(M+H)⁺] 457. HRMS calcd [(M+H)⁺] 457.1710,
45 measured [(M+H)⁺] 457.1719. ¹H NMR (400 MHz, CD₃OD) δ ppm 7.65–7.75 (m, 2H), 7.60 (td, *J* = 4.80,
47 7.96 Hz, 1H), 7.46 (d, *J* = 8.34 Hz, 1H), 7.32 (dd, *J* = 1.77, 8.59 Hz, 1H), 7.17 (dd, *J* = 8.34, 10.36 Hz, 1H),
49 6.15 (s, 1H), 5.20 (s, 2H), 4.53–4.86 (m, 4H), 4.45 (br s, 2H), 3.73–3.86 (m, 2H), 3.65 (s, 2H), 2.43 (s, 3H).

53 Compounds **1h–1q** were prepared by a similar procedure to that described for compound **1g** (Scheme 2).

***N*-[(3-Aminooxetan-3-yl)methyl]-2-(9-methoxy-1,1-dioxido-2,3-dihydro-1,4-benzothiazepin-4(5*H*)-yl)-6-methylquinolin-4-amine (1h)**. A mixture of compound **1g** (20 mg, 0.044 mmol), NaOMe (24 mg, 0.44 mmol) in MeOH (2 mL) was stirred at 100 °C under microwave irradiation for 20 min. After removal of the solvent, the residue was purified by HPLC to afford compound **1h** as a white solid (6 mg, 29%). MS obsd (ESI+) [(M+H)⁺] 469. HRMS calcd [(M+H)⁺] 469.1910, measured [(M+H)⁺] 469.1909. ¹H NMR (400 MHz, CD₃OD) δ ppm 7.67 (s, 1H), 7.52–7.62 (m, 1H), 7.47 (d, *J* = 8.59 Hz, 1H), 7.41 (d, *J* = 7.07 Hz, 1H), 7.31 (dd, *J* = 1.89, 8.46 Hz, 1H), 7.16 (d, *J* = 7.83 Hz, 1H), 5.99 (s, 1H), 5.08 (s, 2H), 4.49–4.63 (m, 4H), 4.31 (t, *J* = 5.56 Hz, 2H), 3.81–3.98 (m, 5H), 3.54 (s, 2H), 2.43 (s, 3H).

***N*-[(3-Aminooxetan-3-yl)methyl]-2-(8-fluoro-1,1-dioxido-2,3-dihydro-1,4-benzothiazepin-4(5*H*)-yl)-6-methylquinolin-4-amine (1i)**. MS obsd (ESI+) [(M+H)⁺] 457. HRMS calcd [(M+H)⁺] 457.1710, measured [(M+H)⁺] 457.1700. ¹H NMR (400 MHz, CD₃OD) δ ppm 7.95 (dd, *J* = 5.18, 8.46 Hz, 1H), 7.64–7.77 (m, 2H), 7.47 (d, *J* = 8.34 Hz, 1H), 7.25–7.43 (m, 2H), 6.20 (s, 1H), 5.19 (br s, 2H), 4.57–4.68 (m, 6H), 3.70 (s, 2H), 3.56–3.67 (m, 2H), 2.44 (s, 3H).

***N*-[(3-Aminooxetan-3-yl)methyl]-2-(8-methoxy-1,1-dioxido-2,3-dihydro-1,4-benzothiazepin-4(5*H*)-yl)-6-methylquinolin-4-amine (1j)**. MS obsd (ESI+) [(M+H)⁺] 469. HRMS calcd [(M+H)⁺] 469.1910, measured [(M+H)⁺] 469.1913. ¹H NMR (400 MHz, CD₃OD) δ ppm 7.82 (d, *J* = 8.34 Hz, 2H), 7.56 (br s, 2H), 7.44 (br s, 1H), 7.18 (d, *J* = 8.59 Hz, 1H), 6.22 (s, 1H), 5.13–5.27 (m, 2H), 4.55–4.74 (m, 4H), 4.50 (br s, 2H), 3.86 (s, 3H), 3.72–3.81 (m, 2H), 3.60–3.71 (m, 2H), 2.46 (s, 3H).

***N*-[(3-Aminooxetan-3-yl)methyl]-6-methyl-2-(8-methyl-1,1-dioxido-2,3-dihydro-1,4-benzothiazepin-4(5*H*)-yl)quinolin-4-amine (1k)**. MS obsd (ESI+) [(M+H)⁺] 453. HRMS calcd [(M+H)⁺] 453.1960, measured [(M+H)⁺] 453.1965. ¹H NMR (400 MHz, CD₃OD) δ ppm 7.82 (d, *J* = 7.83 Hz, 1H), 7.68 (d, *J* = 3.03 Hz, 2H), 7.41 (d, *J* = 6.57 Hz, 1H), 7.33 (d, *J* = 8.59 Hz, 1H), 7.25 (dd, *J* = 1.52, 8.59 Hz, 1H), 6.42 (t, *J* = 5.56 Hz, 1H), 6.19 (s, 1H), 5.05 (br s, 2H), 4.45 (d, *J* = 5.81 Hz, 3H), 4.39 (d, *J* = 6.06 Hz, 3H), 3.60 (t, *J* = 4.55 Hz, 2H), 3.55 (d, *J* = 5.31 Hz, 2H), 2.37 (s, 3H), 2.31 (s, 3H).

1
2
3 ***N*-[(3-Aminooxetan-3-yl)methyl]-2-(8-chloro-1,1-dioxido-2,3-dihydro-1,4-benzothiazepin-4(5*H*)-yl)-**
4 **6-methylquinolin-4-amine (11)**. MS obsd (ESI+) [(M+H)⁺] 473. HRMS calcd [(M+H)⁺] 473.1414,
5 measured [(M+H)⁺] 473.1426. ¹H NMR (400 MHz, CD₃OD) δ ppm 7.88–7.99 (m, 2H), 7.77 (s, 1H), 7.64
6
7 measured [(M+H)⁺] 473.1426. ¹H NMR (400 MHz, CD₃OD) δ ppm 7.88–7.99 (m, 2H), 7.77 (s, 1H), 7.64
8
9 (dd, *J* = 2.27, 8.08 Hz, 1H), 7.53 (d, *J* = 8.59 Hz, 1H), 7.40 (d, *J* = 8.59 Hz, 1H), 6.19 (s, 1H), 5.21 (br s,
10
11 2H), 4.56–4.84 (m, 4H), 4.53 (br s, 2H), 3.75 (s, 2H), 3.68 (br s, 2H), 2.45 (s, 3H).
12
13

14 ***N*-[(3-Aminooxetan-3-yl)methyl]-2-(7-fluoro-1,1-dioxido-2,3-dihydro-1,4-benzothiazepin-4(5*H*)-yl)-**
15 **6-methylquinolin-4-amine (1m)**. MS obsd (ESI+) [(M+H)⁺] 457. ¹H NMR (400 MHz, CD₃OD) δ ppm
16
17 8.02 (dd, *J* = 5.43, 8.72 Hz, 1H), 7.65–7.79 (m, 2H), 7.46 (d, *J* = 8.34 Hz, 1H), 7.33 (d, *J* = 8.84 Hz, 1H),
18
19 7.17 (td, *J* = 2.65, 8.40 Hz, 1H), 6.17 (s, 1H), 5.17 (br s, 2H), 4.41–4.68 (m, 6H), 3.64–3.72 (m, 2H), 3.53–
20
21 3.64 (m, 2H), 2.44 (s, 3H).
22
23
24
25

26 ***N*-[(3-Aminooxetan-3-yl)methyl]-2-(7-methoxy-1,1-dioxido-2,3-dihydro-1,4-benzothiazepin-4(5*H*)-**
27 **yl)-6-methylquinolin-4-amine (1n)**. MS obsd (ESI+) [(M+H)⁺] 469. HRMS calcd [(M+H)⁺] 469.1910,
28
29 measured [(M+H)⁺] 469.1900. ¹H NMR (400 MHz, DMSO-*d*₆) δ ppm 7.79 (d, *J* = 8.84 Hz, 1H), 7.68 (s,
30
31 1H), 7.57 (d, *J* = 2.53 Hz, 1H), 7.34 (d, *J* = 8.59 Hz, 1H), 7.21–7.30 (m, 1H), 6.96 (dd, *J* = 2.65, 8.72 Hz,
32
33 1H), 6.35 (t, *J* = 5.31 Hz, 1H), 6.19 (s, 1H), 5.04 (br s, 2H), 4.39–4.45 (m, 6H), 3.75–3.92 (m, 3 H), 3.45–
34
35 3.62 (m, 4H), 2.37 (s, 3H).
36
37
38
39

40 **4-[4-[(3-Aminooxetan-3-yl)methylamino]-6-methyl-2-quinoly]-1,1-dioxo-3,5-dihydro-2*H*-**
41 **1lambda6,4-benzothiazepin-7-ol (1o)**. A mixture of compound **1m** (20 mg, 0.044 mmol), KOH (24 mg,
42
43 0.44 mmol) in DMSO (2 mL) was stirred at 100 °C under microwave irradiation for 20 min. After removal
44
45 of solvent, the residue was purified by HPLC to afford compound **1o** as a white solid (6 mg, yield 30%).
46
47 MS obsd (ESI+) [(M+H)⁺] 455. HRMS calcd [(M+H)⁺] 455.1753, measured [(M+H)⁺] 455.1745. ¹H NMR
48
49 (400 MHz, CD₃OD) δ ppm 7.77 (d, *J* = 8.59 Hz, 1H), 7.67 (s, 1H), 7.45 (d, *J* = 8.59 Hz, 1H), 7.31 (dd, *J* =
50
51 1.64, 8.46 Hz, 1H), 7.18 (d, *J* = 2.53 Hz, 1H), 6.72 (dd, *J* = 2.27, 8.59 Hz, 1H), 6.19 (s, 1H), 5.03 (s, 2H),
52
53 1.64, 8.46 Hz, 1H), 7.18 (d, *J* = 2.53 Hz, 1H), 6.72 (dd, *J* = 2.27, 8.59 Hz, 1H), 6.19 (s, 1H), 5.03 (s, 2H),
54
55
56
57
58
59
60

1
2
3 4.68 (d, $J = 6.57$ Hz, 2H), 4.61 (d, $J = 6.57$ Hz, 2H), 3.66 (s, 2H), 3.50 (br s, 2H), 3.30 (m, 2H), 2.43 (s,
4 3H).

5
6
7
8 ***N*-[(3-Aminooxetan-3-yl)methyl]-2-(8-methoxy-1,1-dioxido-2,3-dihydro-1,4-benzothiazepin-4(5*H*)-**
9 **yl)quinolin-4-amine (1p)**. MS obsd (ESI+) [(M+H)⁺] 455. HRMS calcd [(M+H)⁺] 455.1753, measured
10 [(M+H)⁺] 455.1762. ¹H NMR (400 MHz, CD₃OD) δ ppm 7.74–7.91 (m, 2H), 7.38–7.58 (m, 3H), 7.03–
11 7.22 (m, 2H), 6.23 (s, 1H), 5.12 (br s, 2H), 4.46–4.70 (m, 6H), 3.81 (s, 3H), 3.70 (s, 2H), 3.52–3.65 (m,
12 2H).

13
14
15
16
17
18
19
20 ***N*-[(3-Aminooxetan-3-yl)methyl]-2-(8-methyl-1,1-dioxido-2,3-dihydro-1,4-benzothiazepin-4(5*H*)-yl)-**
21 **quinolin-4-amine (1q)**. MS obsd (ESI+) [(M+H)⁺] 439. HRMS calcd [(M+H)⁺] 439.1804, measured
22 [(M+H)⁺] 439.1795. ¹H NMR (400 MHz, CD₃OD) δ ppm 7.91 (d, $J = 8.34$ Hz, 1H), 7.84 (d, $J = 7.58$ Hz,
23 1H), 7.60–7.72 (m, 1H), 7.35–7.49 (m, 3H), 7.09 (ddd, $J = 3.03, 5.18, 8.21$ Hz, 1H), 6.52 (t, $J = 5.43$ Hz,
24 1H), 6.22 (s, 1H), 5.06 (br s, 2H), 4.45 (d, $J = 6.06$ Hz, 3H), 4.38 (d, $J = 6.06$ Hz, 3H), 3.61 (t, $J = 4.80$ Hz,
25 2H), 3.56 (d, $J = 5.31$ Hz, 2H), 2.31 (s, 3H).

26
27
28
29
30
31
32
33 ***N*-[(3-Aminooxetan-3-yl)methyl]-3-(1,1-dioxo-3,5-dihydro-2*H*-1lambda6,4-benzothiazepin-4-yl)-7-**
34 **methyl-isoquinolin-1-amine (2a)**. A mixture of 2-(cyanomethyl)-5-methyl-benzoic acid (2 g, 11.4 mmol)
35 and 2,3,4,5-tetrahydro-1lambda6,4-benzothiazepine 1,1-dioxide (**8**, 2.3 g, 11.4 mmol) in DMA (10 mL)
36 was heated with stirring at 170 °C for 2 h. After being cooled to room temperature, the resulting mixture
37 was poured into water. The solid was collected by filtration and washed with ether, dried *in vacuo* to give
38 compound **9a** as a brown solid (1.24 g, yield 31%), which was used for the next step without further
39 purification. MS obsd (ESI+) [(M+H)⁺] 355

40
41
42
43
44
45
46
47
48
49 The compound **9a** (1.24 g, 3.5 mmol) was dissolved in POCl₃ (20 mL). The reaction mixture was stirred
50 under reflux for 5 h. The resulting mixture was poured into ice-water and extracted with EtOAc. The organic
51 layre was dried over Na₂SO₄ and concentrated *in vacuo*. The residue was purified by flash column, eluting
52
53
54
55
56
57
58
59
60

with 10% EtOAc in petroleum ether to give compound **9b** as a brown solid (800 mg, yield 61%). MS obsd (ESI+) [(M+H)⁺] 373.

A mixture of compound **9b** (400 mg, 1.07 mmol), PdCl₂(dppf) (79 mg, 0.107 mmol), dppf (60 mg, 0.107 mmol), *t*-BuONa (206 mg, 2.15 mmol) and 3-(aminomethyl)oxetan-3-amine (110 mg, 1.07 mmol) in 1,4-dioxane (10 mL) was stirred at 150 °C under microwave irradiation for 0.5 h. The resulting mixture was poured into water and extracted with DCM. The organic layer was dried over Na₂SO₄ and concentrated *in vacuo*. The residue was purified by flash column, eluting with a gradient of 0–10% MeOH in DCM to give compound **2a** as a white solid (150 mg, yield 32%). MS obsd (ESI⁺) [(M+H)⁺] 439. HRMS calcd [(M+H)⁺] 439.1804, measured [(M+H)⁺] 439.1805. ¹H NMR (400 MHz, DMSO-*d*₆) δ ppm 7.88 (t, *J* = 7.9 Hz, 2H), 7.77 (s, 1H), 7.61 (dt, *J* = 1.2, 7.5 Hz, 1H), 7.4–7.5 (m, 1H), 7.31 (d, *J* = 8.3 Hz, 1H), 7.22 (d, *J* = 8.4 Hz, 1H), 7.12 (t, *J* = 5.8 Hz, 1H), 6.13 (s, 1H), 4.99 (br s, 2H), 4.47 (d, *J* = 5.7 Hz, 2H), 4.32 (d, *J* = 5.7 Hz, 4H), 3.83 (d, *J* = 5.6 Hz, 2H), 3.59 (t, *J* = 4.9 Hz, 2H), 2.33 (s, 3H).

***N*-[(3-Aminooxetan-3-yl)methyl]-2-(1,1-dioxido-2,3-dihydro-1,4-benzothiazepin-4(5*H*)-yl)-1,6-**

naphthyridin-4-amine (2b). Compound **2b** was prepared in analogue to compound **1a** (Scheme 3). MS obsd (ESI⁺) [(M+H)⁺] 426. HRMS calcd [(M+H)⁺] 426.1600, measured [(M+H)⁺] 426.1592. ¹H NMR (400 MHz, CD₃OD) δ ppm 9.15 (s, 1H), 8.28–8.80 (d, *J* = 6.4 Hz, 1H), 7.95–8.00 (d, *J* = 1.2 Hz, 1H), 7.90–7.95 (d, *J* = 7.2 Hz, 1H), 7.58–7.62 (t, *J* = 0.8 Hz, 1H), 7.40–7.50 (m, 2H), 6.31 (s, 1H), 5.35 (s, 2H), 4.58–4.65 (m, 6H), 3.80 (s, 2H), 3.50–3.60 (t, *J* = 2.8 Hz, 2H).

3-[[[3-(1,1-Dioxo-3,5-dihydro-2*H*-1λ⁶,4-benzothiazepin-4-yl)-1-

naphthyl]amino]methyl]oxetan-3-amine (2c). A mixture of [3-(trifluoromethylsulfonyloxy)-1-naphthyl] 4-methylbenzenesulfonate (5 g, 11.21 mmol), Pd₂(dba)₃ (1 g, 1.12 mmol), dppf (314 mg, 0.56 mmol), *t*-BuONa (1.6 g, 16.82 mmol) and 2,3,4,5-tetrahydro-1λ⁶,4-benzothiazepine 1,1-dioxide (**8**, 2.2 g, 11.21 mmol) in toluene (20 mL) was stirred at 110 °C under microwave irradiation for 0.5 h. The resulting mixture was diluted with water and extracted with EtOAc (50 mL × 3). The organic layer was washed with

1
2
3 brine, dried over Na₂SO₄ and concentrated *in vacuo*. The residue was purified by flash column to give
4
5 compound **11** as a yellow solid (1.38 g, yield 25%).
6
7

8
9 A mixture of compound **11** (1 g, 2.03 mmol), Pd(*t*-Bu₃P)₂ (51.9 mg, 0.102 mmol), Josiphos SL-J003-1 (62
10
11 mg, 0.102 mmol), *t*-BuONa (234 mg, 2.44 mmol) and 3-(aminomethyl)-*N,N*-dibenzylloxetan-3-amine (1.14
12
13 g, 4.06 mmol) in toluene (10 mL) was stirred at 120 °C under Ar with microwave irradiation for 45 min.
14
15 The resulting mixture was diluted with water and extracted with DCM (30 mL × 3). The organic layer was
16
17 washed with brine, dried over Na₂SO₄ and concentrated *in vacuo*. The residue was purified by flash column
18
19 to give compound **12** as a yellow solid (362 mg, yield 29.4%).
20
21

22
23 A mixture of compound **12** (50 mg, 0.083 mmol), palladium hydroxide (10% on carbon, 10 mg) and TFA
24
25 (31 μL) in MeOH (4 mL) was stirred under a hydrogen atmosphere for 5 h. After being basified with
26
27 saturated NaHCO₃, the mixture was extracted with DCM. The organic layer was dried over anhydrous
28
29 Na₂SO₄ and concentrated under reduced pressure. The residue was purified by flash column, eluting with a
30
31 gradient of 0–10% MeOH in DCM to give compound **2c** as a white solid (30 mg, yield 86%). MS obsd
32
33 (ESI+) [(M+H)⁺] 424. ¹H NMR (400 MHz, CD₃OD) δ ppm 7.99 (dd, *J* = 1.26, 7.83 Hz, 1H), 7.79–7.90 (m,
34
35 2H), 7.62 (dt, *J* = 1.26, 7.45 Hz, 1H), 7.52 (d, *J* = 8.34 Hz, 1H), 7.44 (dt, *J* = 1.26, 7.71 Hz, 1H), 7.27 (ddd,
36
37 *J* = 1.14, 6.82, 8.21 Hz, 1H), 7.11 (ddd, *J* = 1.26, 6.88, 8.27 Hz, 1H), 6.44–6.51 (m, 2H), 5.51 (s, 1H), 5.13
38
39 (s, 2H), 4.61–4.71 (m, 4H), 4.59 (s, 2H), 4.38 (br s, 2H), 3.65 (s, 2H).
40
41

42
43 ***N*-[(3-Aminooxetan-3-yl)methyl]-2-(1,1-dioxido-2,3-dihydro-1,4-benzothiazepin-4(5*H*)-yl)-6-**
44
45 **methylquinazolin-4-amine (RO-0529)**. To a solution of 2,4-dichloro-6-methyl-quinazoline (**13a**, 1.0 g,
46
47 4.69 mmol) in MeOH (10 mL) was added 3-(aminomethyl)-*N,N*-dibenzyl-oxetan-3-amine (1.5 g, 5.16
48
49 mmol) and Et₃N (0.1 g, 1 mmol). After being stirred at room temperature overnight, the reaction mixture
50
51 was concentrated *in vacuo* and purified by flash column to give compound **14f** (1.6 g, yield 74%). MS obsd
52
53 (ESI+) [(M+H)⁺] 459. ¹H NMR (400 MHz, CD₃OD) δ ppm 8.01 (s, 1H), 7.68–7.74 (m, 1H), 7.60 (d, *J* =
54
55
56
57
58
59
60

1
2
3 8.4 Hz, 1H), 7.38 (d, $J = 7.0$ Hz, 4H), 7.22–7.30 (m, 4H), 7.15–7.22 (m, 2H), 4.49 (d, $J = 6.6$ Hz, 2H),
4
5 4.32–4.41 (m, 4H), 3.78 (s, 4H), 2.56 (s, 3H).
6
7

8 The mixture of compound **14f** (2 g, 4.4 mmol), 2,3,4,5-tetrahydro-1λ⁶,4-benzothiazepine 1,1-
9 dioxide (**8**, 868 mg, 4.4 mmol) and Et₃N (1.2 mL, 7.6 mmol) in DMF (20 mL) was stirred at 130 °C under
10 microwave irradiation for 2 h. The reaction mixture was diluted with EtOAc (50 mL) and then washed
11 sequentially with water (50 mL × 3) and saturated brine (50 mL). The organic layer was dried over
12 Na₂SO₄, filtered, and then concentrated *in vacuo*. The residue was purified by flash column to give
13 compound **15c** as a white solid (1.4 g, yield 51.4%). MS obsd (ESI⁺) [(M+H)⁺] 620. ¹H NMR (400 MHz,
14 CD₃OD) δ ppm 7.96 (dd, $J = 7.8, 1.1$ Hz, 1H), 7.86–7.91 (m, 1H), 7.69 (s, 1H), 7.59 (td, $J = 1.3, 7.5$ Hz,
15 1H), 7.41–7.49 (m, 2H), 7.36–7.41 (m, 1H), 7.28–7.34 (m, 4H), 7.12–7.24 (m, 6H), 5.19 (br s, 2H), 4.63
16 (d, $J = 6.4$ Hz, 2H), 4.55 (br s, 2H), 4.36–4.45 (m, 4H), 3.85 (s, 4H), 3.42 (br t, $J = 4.7$ Hz, 2H), 2.45 (s,
17 3H).
18
19
20
21
22
23
24
25
26
27
28
29

30 To a solution of compound **15c** (1.4 g, 2.26 mmol) in methanol (50 mL) was added palladium hydroxide
31 (20% on carbon, 200 mg). After being stirred at room temperature overnight under a hydrogen
32 atmosphere, the resulting mixture was filtered. The filtrate was concentrated *in vacuo* and purified by
33 flash column to afford compound **RO-0529** (300 mg, yield 31%). MS obsd (ESI⁺) [(M+H)⁺] 440. HRMS
34 calcd [(M+H)⁺] 440.1756, measured [(M+H)⁺] 440.1751. ¹H NMR (400 MHz, DMSO-*d*₆) δ ppm 7.80–
35 7.93 (m, 4H), 7.62 (t, $J = 7.2$ Hz, 1H), 7.45–7.52 (m, 1H), 7.37 (br d, $J = 7.8$ Hz, 1H), 7.25 (br d, $J = 7.1$
36 Hz, 1H), 5.08 (br s, 2H), 4.49 (br d, $J = 4.0$ Hz, 4H), 4.35 (br s, 2H), 3.71–4.11 (m, 2H), 3.58 (br s, 2H),
37 2.21–2.45 (m, 5H). ¹³C NMR (101 MHz, DMSO-*d*₆) δ 161.06, 156.90, 150.10, 141.10, 138.11, 134.67,
38 133.50, 130.52, 128.09, 127.35, 125.65, 122.27, 110.81, 82.44, 57.49, 55.80, 51.45, 47.15, 44.26, 21.26.
39
40
41
42
43
44
45
46
47
48
49

50 Compounds **3a–3e** were prepared by a similar procedure to that described for compound **RO-0529** (Scheme
51 4).
52
53
54
55
56
57
58
59
60

N1-[2-(1,1-Dioxo-3,5-dihydro-2H-1lambda6,4-benzothiazepin-4-yl)-6-methyl-quinazolin-4-yl]-2-methyl-propane-1,2-diamine (3a). MS obsd (ESI+) [(M+H)⁺] 426. ¹H NMR (400 MHz, CD₃OD) δ ppm 7.99 (d, *J* = 1.9 Hz, 1H), 7.86 (d, *J* = 1.8 Hz, 1H), 7.73 (s, 1H), 7.60 (t, *J* = 2.7 Hz, 1H), 7.40–7.47 (m, *J* = 6.9 Hz, 2H), 7.33–7.36 (m, 1H), 5.20 (s, 2H), 4.58 (br s, 2H), 3.72 (s, 2H), 3.52 (m, 2H), 2.41 (s, 3H), 1.30 (s, 6H).

N-[(1-Aminocyclopropyl)methyl]-2-(1,1-dioxo-3,5-dihydro-2H-1lambda6,4-benzothiazepin-4-yl)-6-methyl-quinazolin-4-amine (3b). MS obsd (ESI+) [(M+H)⁺] 424. HRMS calcd [(M+H)⁺] 424.1807, measured [(M+H)⁺] 424.1807. ¹H NMR (400 MHz, DMSO-*d*₆) δ ppm 7.85–7.96 (m, 2H), 7.76 (br d, *J* = 11.80 Hz, 2H), 7.59–7.66 (m, 1H), 7.43–7.53 (m, 1H), 7.35 (dd, *J* = 1.25, 8.53 Hz, 1H), 7.23 (br d, *J* = 7.78 Hz, 1H), 5.07 (br s, 2H), 4.44 (br s, 2H), 3.57 (br s, 4H), 2.35 (s, 3H), 2.04 (br s, 2H), 0.39–0.68 (m, 4H).

N-[(1-Aminocyclobutyl)methyl]-2-(1,1-dioxo-3,5-dihydro-2H-1lambda6,4-benzothiazepin-4-yl)-6-methyl-quinazolin-4-amine (3c). MS obsd (ESI+) [(M+H)⁺] 438. HRMS calcd [(M+H)⁺] 438.1964, measured [(M+H)⁺] 438.1961. ¹H NMR (400 MHz, CD₃OD) δ ppm 7.98 (d, *J* = 7.6 Hz, 1H), 7.86 (d, *J* = 7.6 Hz, 1H), 7.73 (s, 1H), 7.60 (t, *J* = 7.6 Hz, 1H), 7.32–7.47 (m, 3H), 5.33 (s, 2H), 4.58 (br s, 2H), 3.84 (s, 2H), 3.53 (t, *J* = 4.8 Hz, 2H), 2.41 (s, 3H), 2.21 (m, 2H), 1.97–2.04 (m, 2H), 1.82–1.91 (m, 2H).

N-[(3-Aminooxetan-3-yl)methyl]-2-(1,1-dioxo-3,5-dihydro-2H-1lambda6,4-benzothiazepin-4-yl)quinazolin-4-amine (3d). MS obsd (ESI+) [(M+H)⁺] 426. HRMS calcd [(M+H)⁺] 426.1600, measured [(M+H)⁺] 426.1603. ¹H NMR (400 MHz, CD₃OD) δ ppm 7.93–7.98 (m, 1H), 7.88–7.91 (m, 2H), 7.60–7.64 (m, 1H), 7.51–7.57 (m, 1H), 7.41–7.48 (m, 2H), 7.11–7.15 (m, 1H), 5.24 (s, 2H), 4.54–4.67 (m, 6H), 4.09 (s, 2H), 3.50–3.55 (m, 2H).

N-[(3-Aminooxetan-3-yl)methyl]-6-methyl-2-(1-oxido-2,3-dihydro-1,4-benzothiazepin-4(5H)-yl)quinazolin-4-amine (3e). MS obsd (ESI+) [(M+H)⁺] 424. HRMS calcd [(M+H)⁺] 424.1807, measured [(M+H)⁺] 424.1802. ¹H NMR (400 MHz, CD₃OD) δ ppm 8.01 (s, 1H), 7.79–7.83 (m, 2H), 7.52–7.66 (m, 4H), 5.4–5.45 (d, 1H), 5.10 (br s, 1H), 4.72–4.80 (m, 6H), 4.39 (s, 2H), 3.51 (s, 2H), 2.45 (s, 3H).

1
2
3 **CPE assay.** CPE assay was performed to assess the protective effects of compounds on cell viability. Plates
4 (96-well) were seeded with 6000 Hep-2 cells per well. Cells were infected the next day with RSV at MOI
5 0.02 to produce an approximately 90% cytopathic effect after 5 days. Cells were incubated during this
6 period in the presence or absence of serial dilutions of compounds. The viability of cells was assessed after
7 5 days by CCK-8 (Dojindo Molecular Technologies, Inc.). Results were expressed as 50% effective
8 concentrations (EC₅₀) and 50% cell cytotoxicity (CC₅₀) values. Plaque reduction assays were carried out by
9 infecting Hep-2 cell monolayers with 0.5 ml of 200 PFU/ml of RSV Long strain per well of a 12-well plate
10 with or without the presence of serial diluted compounds. After 2 hours, cells were overlaid with
11 DMEM/F12 containing 4% FBS and 0.55% agarose and compounds. Plates were incubated for 3 days and
12 cells were then fixed with 4% paraformaldehyde for 6 hours. The agarose plugs were removed, and viral
13 plaques were visualized by immunostaining. Cells were blocked with 1× TBS buffer with 1% BSA-0.5%
14 Triton X-100. Plates were then incubated in the presence of a mouse anti-RSV monoclonal antibody (NCL-
15 RSV3; Novocastra) at 1:300 dilution followed by a rabbit anti-mouse horseradish peroxidase-labeled
16 secondary antibody. The plaque staining was developed with 4-chloro-1-naphthol in the presence of
17 hydrogen peroxide, and plaques were counted.

18
19
20
21
22
23
24
25
26
27
28
29
30
31
32
33
34
35
36 ***In vivo* efficacy study.** Six-week-old female BALB/c mice were purchased from Jackson Laboratories and
37 fed a standard diet and water ad libitum. Animals were housed in specific-pathogen-free conditions. The
38 Animal Care Committee of Roche Innovation center China approved the protocol. Animals were
39 anesthetized intraperitoneally with ketamine/xylazine before any intranasal administration. RSV Long
40 strain (5×10⁵ plaque-forming units [PFU] for all animal experiments), drugs, and controls were given in
41 100 μL volumes. Animals were euthanized with CO₂, and lungs were harvested. For histopathologic
42 analysis, the left lower lobe of the lung was removed and inflated with 10% formalin. Specimens were
43 fixed, paraffin embedded, stained, and analyzed.

44
45
46
47
48
49
50
51
52
53
54 **ASSOCIATED CONTENTS**

SUPPORTING INFORMATION

The Supporting Information is available free of charge on the ACS Publications website at XXXX

Detailed experimental procedures for the synthesis of **4b–4h**.

NMR of spectra of compound **RO-0529**.

Pharmacokinetic studies.

Molecular modeling.

Molecular formula strings (CSV).

AUTHOR INFORMATION

Corresponding authors

*Hongying Yun (primary contact and paper writing): Phone: +86 21 28946727. Fax: +86 21 50790293. E-mail: hongying.yun@roche.com.

NOTES

The authors declare no competing financial interest.

ABBREVIATION

RSV, respiratory syncytial virus; RSV F, respiratory syncytia virus fusion protein; BAQ, benzoazepinequinoline; BID, twice a day; COPD, chronic obstructive pulmonary disease; CHF, congestive heart failure; PAMPA, parallel artificial membrane permeability assay; LYSA, lyophilisation solubility assay; ADME, absorption, distribution, metabolism, and excretion; mlLogD, machine learning LogD; MW, microwave irradiation; PPB, plasma protein binding; SDPK, single-dose pharmacokinetics; HPLC, high performance liquid chromatography; IPA, isopropanol; PD, pharmacodynamics; PK, pharmacokinetic.

ACKNOWLEDGEMENTS

We are grateful to Qingshan Gao, Ying Ji, Wei Li, Wenzhi Chen, Yang Lu, Yongguo Li, Liqin Chen, Peilan Ding, Wei Zhang, Hongxia Qiu, Yi Zhang, Yuxia Zhang, Sheng Zhong, Kai Sun, Rong Zhao,

1
2
3 Shuang Ren, Jian Xin and Rong Zhao for purification of the final compounds and the analytical assistance.
4
5 We thank the process group, including Jin She and Yi Ren, for their assistance with large scale synthesis
6
7 campaigns. We also would like to thank Kunlun Xiang for CPE, plaque reduction and resistant mutation
8
9 selection assays. In addition, we thank WuXi AppTec and ChemPartner chemists for working together with
10
11 us in some building block synthesis.
12
13

14 REFERENCE

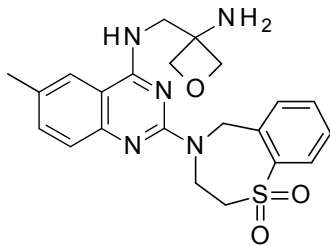
- 15
16
17 1. Borchers, A. T.; Chang, C.; Gershwin, M. E.; Gershwin, L. J. Respiratory syncytial virus-a
18 comprehensive review. *Clin. Rev. Allergy Immunol.* **2013**, *45*, 331–379.
- 19
20 2. Piedimonte, G.; Perez, M. K. Alternative mechanisms for respiratory syncytial virus (RSV) infection
21 and persistence: could RSV be transmitted through the placenta and persist into developing fetal lungs?
22
23 *Curr. Opin. Pharmacol.* **2014**, *16*, 82–88.
- 24
25 3. Wright, M.; Piedimonte, G. Respiratory syncytial virus prevention and therapy: past, present, and
26 future. *Pediatr. Pulmonol.* **2011**, *46*, 324–347.
- 27
28 4. Sigurs, N. Epidemiologic and clinical evidence of a respiratory syncytial virus reactive airways disease
29 link. *Am. J. Crit. Care Med.* **2001**, *163* (no 3), S2–6.
- 30
31 5. Falsey, A. R.; Hennessey, P. A.; Formica, M. A.; Cox, C.; Walsh, E. E. Respiratory syncytial virus
32 infection in elderly and high-risk adults. *N. Engl. J. Med.* **2005**, *352* (17), 1749–1759.
- 33
34 6. Boeckh, M.; Englund, J.; Li, Y.; Miller, C.; Cross, A.; Fernandez, H.; Kuypers, J.; Kim, H.; Gnann, J.;
35 Whitley, R. Randomized controlled multicenter trial of aerosolized ribavirin for respiratory syncytial
36 virus upper respiratory tract infection in hematopoietic cell transplant recipients. *Clin. Infect. Dis.* **2007**,
37
38 *44*, 245–249.
- 39
40 7. Ventre, K.; Randolph, A. G. Ribavirin for respiratory syncytial virus infection of the lower respiratory
41 tract in infants and young children. *Cochrane Database Syst. Rev.* **2010**, DOI: 10.1002/14651858,
42
43 CD000181.
44
45
46
47
48
49
50
51
52
53
54
55
56
57
58
59
60

- 1
2
3 8. The Impact-RSV Study Group. Palivizumab, a humanized respiratory syncytial virus monoclonal
4 antibody, reduces hospitalization from respiratory syncytial virus infection in high-risk infants.
5
6 *Pediatrics* **1998**, *102*, 531–537.
7
- 8
9 9. Zhao, X.; Singh, M.; Malashkevich, V. N.; Kim, P. S. Structural characterization of the human
10 respiratory syncytial virus fusion protein core. *PNAS*. **2000**, *97*, 14172–14177.
11
- 12
13 10. Ding, W. D.; Mitsner, B.; Krishnamurthy, G.; Aulabaugh, A.; Hess, C. D.; Zaccardi, J.; Cutler, M.;
14 Feld, B.; Gazumyan, A.; Raifeld, Y.; Antonia Nikitenko, A.; Lang, S. A.; Gluzman, Y.; O'Hara, B.;
15 Ellestad, G. A. Novel and specific respiratory syncytial virus inhibitors that target virus fusion. *J. Med.*
16
17 *Chem.* **1998**, *41*, 2671–2675.
18
- 19
20 11. Andries, K.; Moeremans, M.; Gevers, T.; Willebrords, R.; Sommen, C.; Lacrampe, J.; Janssens, F.;
21 Wyde, P. R. Substituted benzimidazoles with nanomolar activity against respiratory syncytial virus.
22
23 *Antiviral Res.* **2003**, *60*, 209–219.
24
- 25
26 12. Bonfanti, J. F.; Meyer, C.; Doublet, F.; Fortin, J.; Muller, P.; Queguiner, L.; Gevers, T.; Janssens, P.;
27 Szel, H.; Willebrords, R.; Timmerman, P.; Wuyts, K.; van Remoortere, P.; Janssens, F.; Wigerinck, P.;
28
29 Andries, K. Selection of a respiratory syncytial virus fusion inhibitor clinical candidate. 2. Discovery
30
31 of a morpholinopropylaminobenzimidazole derivative (TMC353121). *J. Med. Chem.* **2008**, *51*,
32
33 875–896.
34
- 35
36 13. Yu, K. L.; Sin, N.; Civiello, R. L.; Wang, X. A.; Combrink, K. D.; Gulgeze, H. B.; *et al.* Respiratory
37
38 syncytial virus fusion inhibitors. Part 4: Optimization for oral bioavailability. *Bioorg. Med. Chem. Lett.*
39
40 **2007**, *17*, 895–901.
41
- 42
43 14. Sun, Z.; Pan, Y.; Jiang, S.; Lu, L. Respiratory syncytial virus entry inhibitors targeting the F protein.
44
45 *Viruses* **2013**, *5*, 211–225.
46
- 47
48 15. Stevens, M.; Rusch, S.; Huntjens, D.; Lounis, N.; Mari, N. K.; Remmerie, B.; Roymans, D.; Koul A.;
49
50 Verloes, R.; DeVincenzo, J.; Kim, Y.; Harrison, L.; Meals, E. A.; DeVincenzo, J.; DeVincenzo, J.;
51
52 Boyers, A.; Fok-Seang, J., Antiviral activity of oral JNJ-53718678 in healthy adult volunteers
53
54
55
56
57
58
59

- 1
2
3 challenged with respiratory syncytial virus: a placebo-controlled study. *J. Infect. Dis.* **2018**, *218*(5),
4 748–756.
5
6
- 7 16. Mackman, R. L.; Sangi, M.; Sperandio, D.; Parrish, J. P.; Eisenberg, E.; Perron, M.; Hui, H.; Zhang,
8 L.; Siegel, D.; Yang, H.; Saunders, O.; Booramra, C.; Lee, G.; Samuel, D.; Babaoglu, K.; Carey, A.;
9 Gilbert, B. E.; Piedra, P. A.; Strickley, R.; Iwata, Q.; Hayes, J.; Stray, K.; Kinkade, A.; Theodore, D.;
10 Jordan, R.; Desai, M.; Cihlar, T. Discovery of an oral respiratory syncytial virus (RSV) fusion inhibitor
11 (GS-5806) and clinical proof of concept in a human RSV challenge study. *J. Med. Chem.* **2015**, *58*,
12 1630–1643.
13
14
- 15 17. Perron, M.; Stray, K.; Kinkade, A.; Theodore, D.; Lee, G.; Eisenberg, E.; Sangi, M.; Gilbert, B. E.;
16 Jordan, R.; Piedra, P. A.; Toms, G. L.; Mackman, R.; Cihlar, T. GS-5806 inhibits a broad range of
17 respiratory syncytial virus clinical isolates by blocking the virus-cell fusion process. *Antimicrobial*
18 *Agents and Chemotherapy* **2016**, *60*, 1264-1273.
19
20
- 21 18. DeVincenzo, J.; Tait, D.; Oluwayi, O.; Mori, J.; Thomas, E.; Mathews, N.; Harland, R.; Cockerill, S.;
22 Powell, K.; Littler, E. Safety and efficacy of oral RV521 in a human respiratory syncytial virus (RSV)
23 phase 2a challenge study. B14 late breaking clinical trials and first reports in asthma and COPD.
24 *American Journal of Respiratory and Critical Care Medicine* **2018**, *197*, A7715.
25
26
- 27 19. Douglas, J. L.; Panis, M. L.; Ho, E.; Lin, K. Y.; Krawczyk, S. H.; Grant, D. M.; Cai, R.; Swaminathan,
28 S.; Cihlar, T. Inhibition of respiratory syncytial virus fusion by the small molecule VP-14637 via
29 specific interactions with F protein. *J. Virol.* **2003**, *77*, 5054–5064.
30
31
- 32 20. Xiufang Zheng, Chungeng Liang, Lisha Wang, Baoxia Wang, Yongfu Liu, Song Feng, Jim Zhen Wu,
33 Lu Gao, Lichun Feng, Li Chen, Tao Guo, Hong C. Shen, and Hongying Yun “Discovery of
34 benzoazepinequinoline (BAQ) derivatives as novel, potent, orally bioavailable respiratory syncytial
35 virus fusion inhibitors” *J. Med. Chem.* **2018**, *61* (22), 10228-10241.
36
37
- 38 21. Ark Biosciences; Viral Inhibition in Children for Treatment of RSV (VICTOR). *ClinTrials.gov* **2016**,
39 NCT02654171.
40
41
42
43
44
45
46
47
48
49
50
51
52
53
54
55
56
57
58
59
60

- 1
2
3 22. Battles, M. B.; Langedijk, J. P.; Furmanova-Hollenstein, P.; Chaiwatpongsakorn, S.; Costello, H. M.;
4
5 Kwanten, L.; Vranckx, L.; Vink, P.; Jaensch, S.; Jonckers, T. H. M.; Koul, A.; Arnoult, E.; Peeples, M.
6
7 E.; Roymans, D.; McLellan, J. S. Molecular mechanism of respiratory syncytial virus fusion inhibitors.
8
9 *Nat. Chem. Biol.* **2016**, *12*, 87–93.
10
11 23. Ark Biosciences; Safety, Tolerability and PK Study of AK-0529 in Healthy Human. *ClinTrials.gov*
12
13 2014, NCT02297594.
14
15 24. Ark Biosciences; A Study of AK0529 to Evaluate Pharmacokinetics and Safety in Chinese Healthy
16
17 Volunteers. *ClinTrials.gov* 2017, NCT03322800.
18
19 25. Ark Biosciences; A Study to Evaluate the Pharmacokinetics, Metabolism, and Excretion of AK-0529.
20
21 *ClinTrials.gov* 2018, NCT03400995.
22
23
24
25
26
27
28
29
30
31
32
33
34
35
36
37
38
39
40
41
42
43
44
45
46
47
48
49
50
51
52
53
54
55
56
57
58
59
60

Table of Contents graphic

**RO-0529 (AK0529)**RSV CPE EC₉₀/CC₅₀: 0.005/ >100 μM